International Journal of Robotics and Automation (IJRA)

ISSN : 2180-1312

Volume 1, Issue 5

Number of issues per year: 6

International Journal of Robotics and Automation (IJRA)

Volume 1, Issue 5, 2011

Edited By
Computer Science Journals
www.cscjournals.org

International Journal of Robotics and Automation (IJRA)

Book: 2011 Volume 1, Issue 5
Publishing Date: 08-02-2011
Proceedings
ISSN (Online): 2180-1312

IJRA Journal is a part of CSC Publishers
http://www.cscjournals.org

Published in Malaysia

Typesetting: Camera-ready by author, data conversation by CSC Publishing Services – CSC Journals, Malaysia

CSC Publishers

Editorial Preface

Robots are becoming part of people's everyday social lives - and will increasingly become so. In future years, robots may become caretaking assistants for the elderly or academic tutors for our children, or medical assistants, day care assistants, or psychological counselors. Robots may become our co-workers in factories and offices, or maids in our homes. It is the fourth issue of volume first of International Journal of Robotics and Automation (IJRA). IJRA published six times in a year and it is being peer reviewed to very high International standards.

IJRA looks to the different aspects like sensors in robot, control systems, manipulators, power supplies and software. IJRA is aiming to push the frontier of robotics into a new dimension, in which motion and intelligence play equally important roles. IJRA scope includes systems, dynamics, control, simulation, automation engineering, robotics programming, software and hardware designing for robots, artificial intelligence in robotics and automation, industrial robots, automation, manufacturing, and social implications etc. IJRA cover the all aspect relating to the robots and automation.

The IJRA is a refereed journal aims in providing a platform to researchers, scientists, engineers and practitioners throughout the world to publish the latest achievement, future challenges and exciting applications of intelligent and autonomous robots. IJRA open access publications has greatly speeded the pace of development in the robotics and automation field. IJRA objective is to publish articles that are not only technically proficient but also contains state of the art ideas and problems for international readership.

In order to position IJRA as one of the top International journal in signal processing, a group of highly valuable and senior International scholars are serving its Editorial Board who ensures that each issue must publish qualitative research articles from International research communities relevant to signal processing fields.

IJRA editors understand that how much it is important for authors and researchers to have their work published with a minimum delay after submission of their papers. They also strongly believe that the direct communication between the editors and authors are important for the welfare, quality and wellbeing of the Journal and its readers. Therefore, all activities from paper submission to paper publication are controlled through electronic systems that include electronic submission, editorial panel and review system that ensures rapid decision with least delays in the publication processes.

To build its international reputation, we are disseminating the publication information through Google Books, Google Scholar, Directory of Open Access

Journals (DOAJ), Open J Gate, ScientificCommons, Docstoc and many more. Our International Editors are working on establishing ISI listing and a good impact factor for IJRA. We would like to remind you that the success of our journal depends directly on the number of quality articles submitted for review. Accordingly, we would like to request your participation by submitting quality manuscripts for review and encouraging your colleagues to submit quality manuscripts for review. One of the great benefits we can provide to our prospective authors is the mentoring nature of our review process. IJRA provides authors with high quality, helpful reviews that are shaped to assist authors in improving their manuscripts.

Editorial Board Members
International Journal of Robotics and Automation (IJRA)

Editorial Board

Table of Content

Volume 1, Issue 5, December 2011

Pages

Determination of the Operational Parameters of a Planar Robot with Three Joints

Muharrem Zeytinoğlu mzeytin@uludag.edu.tr
Department of Biosystems Engineering
Faculty of Agriculture
Uludağ University
Bursa, 16059, Turkey

Halil Ünal hunal@uludag.edu.tr
Department of Biosystems Engineering
Faculty of Agriculture
Uludağ University
Bursa, 16059, Turkey

Abstract

Robots are currently made in numerous types and are used in diverse roles such as production lines, daily living activities and some security fields. These types of robots are well designed and successfully applied in many areas requiring high sensitivity and stability. The aim of this study was to determine the optimum values of several operational parameters for a planar robot with respect to robot design and construction. With this aim, a small planar robot with a three-jointed arm activated by hydraulic cylinders in each segment was evaluated using a technical design drawing. The arm motions of the planar robot are rotary and parallel within a vertical plane. The resulting optimal operational parameters of the planar robot were determined as starting and target positions of 31.5 cm and 55 cm, respectively, on the x-axis and 17.18 cm and 118.44 cm on the y–axis. Time-position and time-velocity graphs were constructed corresponding to the orbit-planning parameters, resulting in Cartesian velocities for the terminal processor of 13.98 m/sec on the x-axis and 20.16 m/sec on the y-axis at 1.5 seconds after initiation. The maximum power consumption of the robot was determined as 1 kW according to the outer load and arm weights.

Keywords: Planar robot, Orbit-planning parameter, Cartesian velocity, Kinematic analysis.

1. INTRODUCTION

Planar robots are well recognized as practical robots; they are generally of linear construction and operate on a fixed route in a process implemented by rotating or sliding in parallel to a given plane. These types of robots have mostly been applied to linear activities such as the rapid lifting, carrying, and placement of various parts [4]. The vibrational rate of planar robots is lower than for other kinds of more versatile robots because planar robots are required to perform fewer operations; therefore, planar robots have an important advantage with respect to sensitivity and stability.

Currently, a number of different types of planar robots are required in industrial, agricultural, and security areas as well as daily living activities; they are constructed in a diversity of designs and dimensions for these different applications [9]. In this study, a planar robot was designed from a technical drawing (Figure 1) with three arm segments and three joints. Each segment is moved by a hydraulic cylinder; the motion of the arm segments is in parallel to a

plane, and the entire arm rotates. The planar robot also has a terminal processor, i.e., a hook attached to its end point, which moves linearly and rotates in the same plane between the starting point, which is at the inactive position of the hydraulic cylinders, and the target point, which is at the fully actuated position of the hydraulic cylinders. The inverse analysis can be made by considering the planar robot to work in the opposite direction, i.e., by swapping the starting and target points. The planar robot was designed to lift a specific load. The operational parameters investigated were the starting and target positions, the time-position and time-velocity relations, the Cartesian velocities of the terminal processor and the maximum power consumption of the robot, which in turn depend on the robot design parameters. The optimal operational parameters were determined by means of several analytical methods; to this end, time-position and time-velocity graphs were constructed from the results of a kinematic analysis of the robot [5]. The motion of the terminal processor was the main factor in the kinematic analysis, and its motion is determined by the configuration of the joint points in the action plane. The motion can be configured into various paths, such as a linear, circular, sinusoidal or irregular path [1]. Kinematic analysis was performed by orbit planning, which is necessary to ensure that robot motion is steady and controllable, without vibration or deflection from the working space [3].

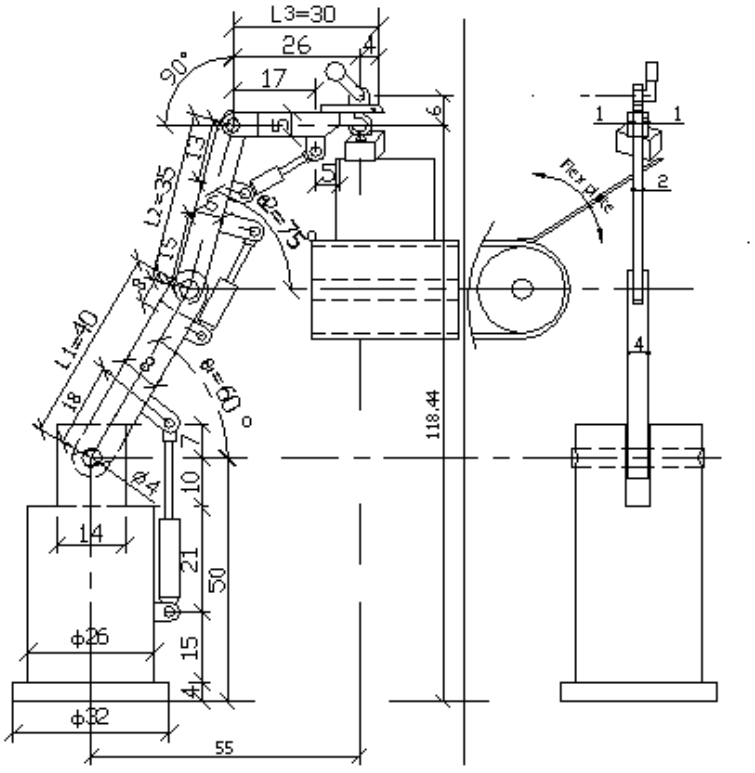

FIGURE 1: Views of the planar robot with three joints in the target position; all dimensions are in cm

Orbit planning for robots can be done using either of two methods: the Cartesian and joint-space methods. In this study, the joint-space method was used; here, each joint was considered to be independent of the others, and therefore, the velocity of each joint was different in the orbit planning. In this model, the hydraulic-cylinder pressures and capacities are also different when reaching the required position of the terminal processor. A detailed view of the orbit planning was obtained through a third-degree polynomial equation, and the time-position and time-velocity relations were determined from the solutions of the polynomial equation 5. Determining the Cartesian velocities from the operational parameters of the robot is very important with respect to the level of swing inertia encountered during the lifting of a specific load. The working velocity and arm-segment lengths of the robot are the determining factors of the Cartesian velocities. The maximum robot power consumption was calculated

corresponding to the planar velocities of the solid materials [6]. The final results for the optimum operational parameters are given in Table 3.

As shown in Figure 1, the robot under study has a base frame constructed of thick-walled steel tubing that is located on the floor at one side. The terminal processor has a top working weight combined with a hook; these are restrained by a stop in the starting position of the lifting operation. As the lifting operation concludes, the hook is cleared on the reverse side by the balanced movement of the top weight, facilitating the release of the load from the hook, thus leaving the load on the conveyor band in the target position. The hook is located at the end of the third arm segment, and its weight is considered as equal to the empty volume of the third arm segment. The hook-lifted load is 40 N, and this weight was added to the weight of arm Segment 3 in the calculation of the robot's power consumption.

2. DETERMINATION OF THE ROBOT OPERATIONAL PARAMETERS

The operating parameters were determined for the robot arm shown in Figure 1. The analytical methods used to determine the robot operational parameters are given below.

2.1. Starting and Target Positions

Each position was determined with respect to the reference axis of the base of the frame as shown in Figures 1 and 2.

The starting position can be expressed as:

$$P_X = L_1 + L_2.C(60^o) - L_3 \quad (1)$$

$$P_Y = 50 - L_2.S(60^o) \quad (2)$$

where:

PX : Horizontal distance between the reference axis of the frame base and the terminal processor (cm)

PY : Vertical distance between the reference axis of the frame base and the terminal processor (cm)

L1, L2, and L3 : Lengths of robot arm Segments 1, 2 and 3, respectively (cm)

The target position can be expressed as:

$$P_X = L_3 + (L_2.C(\theta_2) + L_1.C(\theta_1)). + L_1.C(\theta_1) \quad (3)$$

$$P_Y = 50 + L_2.S(\theta_2) + L_1.S(\theta_1) \quad (4)$$

where:

θ_1, θ_2 : Angles of robot arm Segments 1 and 2 (degrees)

50 : Height of frame base (cm)

2.2. Orbit Planning By the Joint-Space Method

Orbital planning was performed using several polynomial equations describing the robot's motions. Third-degree or higher polynomials are often used in robot designs using the joint-space method. In this study, a third-order polynomial equation and a cubic orbit were used to represent position as a function of time. Position angles and velocities, which are related to the starting and target positions, were the main variables taken into consideration in the polynomial. Here the starting angle and target position are denoted by θ_0, θ_f, respectively, and the corresponding velocities are given by $\theta^{'} = 0, \theta^{'}(t_f) = 0$. With these conditions, the starting and target positions are not active; therefore, the velocities and angles of both of these positions were set at zero.

The third-order polynomial equation can be expressed as:

$$\theta_{(t)} = S_0 + S_1 t + S_2 t^2 + S_3 t^3 \quad (5)$$

where:

S0 : (θ0) Coefficient of starting position in the inactive condition
S1, S2, S3 : Polynomial coefficients
t : Time (seconds)

The velocities and accelerations of the robot joints were determined by taking the first and second derivatives of Equation 5, respectively.

The first derivative of Equation 5 can be expressed as:

$$\theta'_{(t)} = S_1 + 2S_2 t + 3S_3 t^2 \quad (6)$$

where:
S1, S2, S3 : Polynomial coefficients
t : Time (sec)

The polynomial coefficients can be determined from Equation 5 corresponding to specific angles of the robot. The coefficient S1 is zero in Equation 5, representing the starting time.

The polynomial coefficient S_2 can be expressed as:

$$S_2 = \frac{3}{t_{f^2}} \cdot (\theta_f - \theta_0) \quad (7)$$

where:
t_f = Time at target position (sec)
θ_f = Angle at target position (degrees)
θ_0 = Angle at starting position (degrees)

The polynomial coefficient S_3 can be expressed as:

$$S_3 = -\frac{2}{t_{f^3}} \cdot (\theta_f - \theta_0) \quad (8)$$

The robot processing time (t) between the starting and target positions in the stationary frame was taken as four seconds. The maximum joint angles corresponding to the robot shown in Figure 1 were 60º, 75º and 45º, respectively, for Joints 1, 2 and 3. Robot joint angles are inactive conditions in the starting position; therefore, the joint velocities are zero at the starting position, as shown in Figure 2. The joint positions are given at a time of 1.5 sec in the same figure. Time-position and time-velocity graphs were determined from the results of the polynomial equations, as shown in Figure 3. The maximum velocity of each joint was at t = 2 sec, and the results for the joint positions and velocities for the times of 1.5 and 2 sec, also derived from Figure 3, are given in Table 1.

The Cartesian velocities of Joint 3 were determined from the velocities of Joints 1 and 2 in a two-dimensional plane; there was a large swing velocity at t = 1.5 sec, as shown in Table 1.

Position times (sec.)		**Starting**	**Target**	**1.5 sec.**	**2 sec.**
Joint 1	Position (Degree)	0	60	18.98	30
	Velocity (Degree/sec.)	0	0	21.10	22.50
Joint 2	Position (Degree)	120	75	23.72	37.49
	Velocity (Degree/sec.)	0	0	26.36	28.12
Joint 3	Position (Degree)	60	45	14.23	22.50
	Velocity (Degree/sec.)	0	0	15.82	16.87

TABLE 1: Positions and velocities of joints at the times of 1.5 and 2 sec.

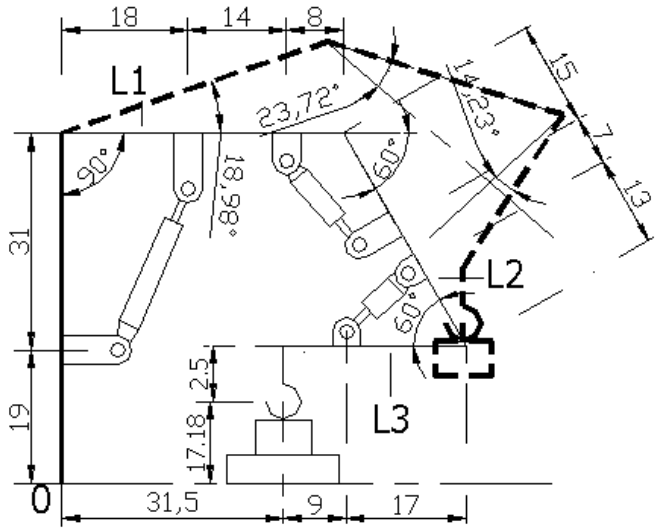

FIGURE 2: Profile view of the planar robot with three joints in the starting position and in a lifting position at a time of 1.5 sec; all dimensions are in cm

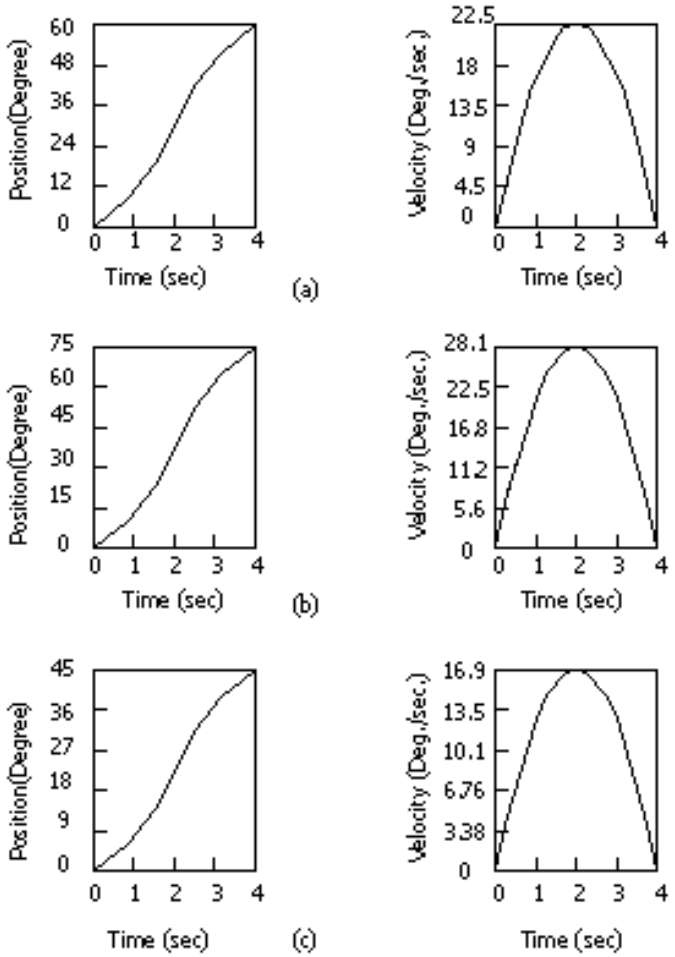

FIGURE 3: Graphs of position and velocity versus time for a) Joint 1, b) Joint 2 and c) Joint 3

The Cartesian velocities can be expressed as:

$$ {}^{0}\begin{bmatrix} V_X \\ V_Y \end{bmatrix}_3 = \begin{bmatrix} -L_1.S.\theta_1 - L_2.S\theta_{12} & -L_2.S\theta_{12} \\ L_1.C\theta_1 + L_2.C\theta_{12} & L_2.C\theta_{12} \end{bmatrix} . \begin{bmatrix} \theta_1^{'} \\ \theta_2^{'} \end{bmatrix} \quad (9) $$

where:

V_X, V_Y : Cartesian velocities of Joint 3 (m/sec)

L_1, L_2 : Lengths of robot arm Segments 1 and 2 (m)

$S\theta_{12} = S(\theta_1 + \theta_2)$: Sine representation of the joint angles in Equation 9

$C\theta_{12} = C(\theta_1 + \theta_2)$: Cosine representation of the joint angles in Equation 9

$\theta_1^{'}, \theta_2^{'}$: Joint velocities at t = 1.5 sec

The Cartesian velocities can be expressed for the robot in reverse as:

$$ {}^{0}\begin{bmatrix} V_X \\ V_Y \end{bmatrix}_3 = \begin{bmatrix} -L_3.S\theta_3 - L_2.S\theta_{32} & -L_2.S\theta_{32} \\ L_3.C\theta_3 + L_2.C\theta_{32} & L_2.C\theta_{32} \end{bmatrix} . \begin{bmatrix} \theta_3^{'} \\ \theta_2^{'} \end{bmatrix} \quad (10) $$

where:

VX, VY : Cartesian velocities of Joint 2 (m/sec)

L3, L2 : Lengths of robot arm Segments 2 and 3 (m)

$S\theta_{32} = S(\theta_3 + \theta_2)$: Sine representation of the joint angles in Equation 10

$C\theta_{32} = C(\theta_3 + \theta_2)$: Cosine representation of the joint angles in Equation 10

$\theta_3^{'}, \theta_2^{'}$: Joint velocities at t = 1.5 sec

The Cartesian velocities of the terminal processor were determined by taking the normal and reverse of the velocity matrices according to Equations 9 and 10, and the difference in the velocities of Joint 3 and Joint 2 was thus determined. Subsequently, this difference in velocities was divided by four because the mean velocities of Joints 3 and 2 and the mean velocities of the reverse kinematics give the pointedlly coordinate velocities of the terminal processor.

2.3. Robot Power Consumption

The kinetic energy of the robot arm can be expressed as [2], [8]***:***

$$ K = \frac{1}{2}\sum_{i=1}^{3} m_1.V_1^2 + \frac{1}{2}\sum_{i=1}^{3} I.\theta_a^{'\,2} \quad (11) $$

where:

K : Kinetic energy (Hp-h)

m_1, m_2, and m_3 : Masses of arm segments 1, 2 and 3 (N sec^2/m) (mass of Segment 3 (m_3) is combined with a specific load)

V_1, V_2, and V_3 : Maximum linear velocities of each arm segment (m/sec)

I_1, I_2, and I_3 : Inertial moments of each arm segment (N sec^2 m),

$\theta_a^{'}$: Angular velocities of each joint $\theta'_{a1}, \theta'_{a2}, \theta'_{a3}$ (r/sec)

The inertial moment of each arm can be expressed as [6], [8]***:***

$$ I = \frac{W}{g}.\frac{l^2}{3} \quad (12) $$

where:

W : Weight of each arm segment (the weight of the third arm segment is combined with a specific load) (N)

g : Acceleration of gravity (m/sec2)

l : Length of each arm segment (m)

The angular velocity of each joint can be expressed as [7]***:***

$$\theta'_a = \omega = \frac{V}{r} \qquad (13)$$

where:
V : Maximum linear velocity of each arm segment (m/sec)
r : Length of each arm segment; r = l (m)

The dimensions of the arm segments are given in Figure 4; the arm material is “ST 42” steel, and the arm-segment weights were computed according to the arm dimensions. The results of the arm-segment weights are given in Table 2.

Robot arm number	Weights (N)
Arm 1	105
Arm 2	37
Arm 3	27

TABLE 2: Weights of linkage arms.

First, the kinetic energy was calculated for the maximum power consumed (P) per second from Equation 11, then the kinetic-energy result was multiplied by 3,600 seconds per hour and divided by the coefficient of 75 to yield the robot power consumption [11].

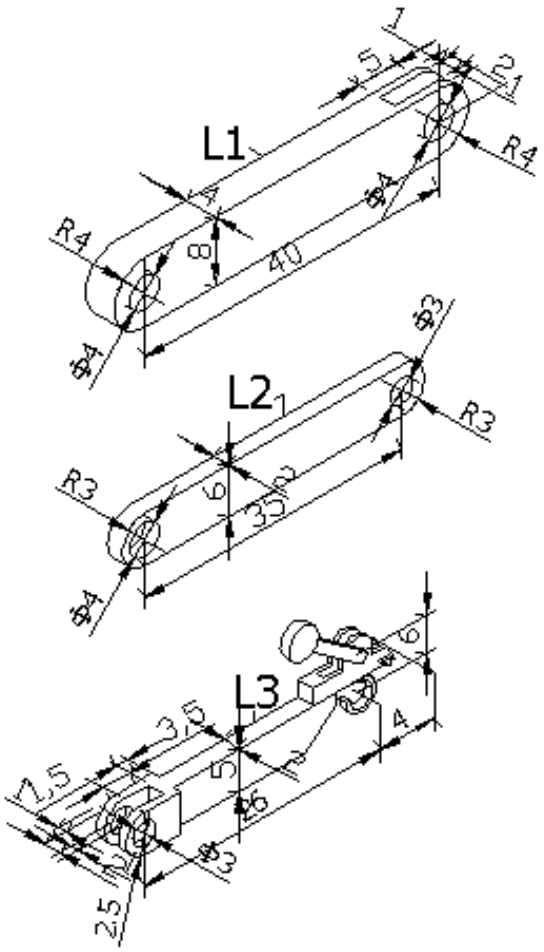

FIGURE 4: Diagrams of linkage arms and their dimensions (in cm)

3. RESULTS AND DISCUSSION

The results of the study are summarized in Table 3.

Parameters	Symbol	Results
Starting position (cm)	Px Py	31.5 17.18
Target position (cm)	Px Py	55 118.44
Maximum velocity of joints (Degree/sec.)	Joint 1 Joint 2 Joint 3	22.5 28.12 16.87
Cartesian velocity of terminal processor at 1.5 sec. (m/sec.)	Vx Vy	13.98 20.16
Cartesian velocities in reverse of terminal processor at 1.5 sec. (m/sec.)	Vx Vy	10.18 16.18
Max.linear velocities of robot arms (m/sec.)	Arm 1 Arm 2 Arm 3	0.157 0.171 0.088
Max.robot power consumtion (kW)	P	1

TABLE 3: Results of study related to the planar robot with three-joint

As evidenced by the dimensions of the positions in Table 3, the working space of the planar robot was relatively small compared to the base area, and the size of the load was small compared to the robot's weight. In these conditions, designs for the construction of larger robots with more power can be achieved via the simulation of planar robots working by hydraulic power.

The motion of the planar robots is linear and rotary in the same plane, and the terminal processor may travel a long distance because of the rotary path in the working space; therefore, the Cartesian velocities and robot power consumption are increased according to the shape of the rotary path. Another important factor causing increased power consumption is the short operational time of four seconds. Robot joint velocities were determined according to the operating time, which was taken into consideration as a basis in reaching the target position of the robot terminal processor. To this end, time-position and time-velocity graphics were determined as operational parameters (Figure 3). High velocities were determined for Joint 2 of the robot: 26.36 and 28.12 degrees/sec at the times of 1.5 and 2 seconds, respectively. The corresponding Cartesian velocities were determined as VX = -13.98 and VY = 20.16 m/sec at the time of 1.5 seconds, as shown in the Table 3. The Cartesian velocities can be considered to be at a moderate level with respect to the swing of the terminal processor with a weight of 40 N or less. In the case of a new design for a planar robot of greater dimensions and load capacity, revisions should be made to control the swing of the bigger load due to the increasing Cartesian velocities. Maximum robot power consumption was determined to be 1 kW. Generally, the power can be considered to the optimal level corresponding to a small working space. Consequently, the maximum Cartesian velocities and robot power are related to the construction dimensions and the operating time; these important parameters should thus be taken into consideration in other planar-robot designs.

4. CONCLUSION

The robot under study is considered fairly small for a large activity area and working with heavy loads. In contrast, this type of robot can be considered on the larger side for smaller areas working with a minimal activity and a light load. Designs for the construction of planar robots working on a small scale have been limited by the availability of auxiliary equipment, e.g., miniature hydraulic components, which are not generally produced in nonstandard specifications, except for the other driver unit. Generally, large constructions related to larger-scale planar robots can be designed easily and suitably for heavy industrial applications, agricultural harvesting and daily living activities. The robot in this study can be considered as

being in the middle scale of construction and at a normal level of power consumption on the basis of the scaling criteria. Consequently, the parameters resulting from this study are applicable to the design and construction of planar robots driven by hydraulic cylinders, especially in large activity areas at average operating velocities; for heavier loads, they can be chosen as initial parameters for future designs.

Nomenclature

Px Robot starting and target positions in the x direction (cm)
Py Robot starting and target positions in the y direction (cm)
υ(t) Polynomial indicator
υ'(t) Joint-velocity indicator
S2, S3 Polynomial coefficients
t Time (sec)
υf Angle of target position (degrees)
υoo Angle of starting position (degrees)
tf Time at target position (sec)
Vx Cartesian velocity in the x direction (m/sec)
Vy Cartesian velocity in the y direction (m/sec)
L1, L2 Length of robot arm Segments 1 and 2 (m)
Sυ1,2 Sine representation of the joint angles
Cυ1,2 Cosine representation of the joint angles
υ'1 , υ'2 Velocities of Joints 1 and 2 (m/sec)
K Kinetic energy (Nm)
M Mass of arm segment (N sec2/m)
V Maximum velocity of arm segment (m/sec)
I Inertial moment of arm segment (N sec2 m)
υα' Angular velocity of joint (rad/sec)
W Weight of arm segment (N)
g Acceleration of gravity (m/sec2)
r = l Length of arm segment (m)
P Maximum robot power consumption (kW)

5. REFERENCES

1. Z. Bingül and S. Kücük, "Technique of robot I" Birsen Publisher, Code No: Y.0029, İstanbul 2005.

2. A. Egrisögüt and R. Kazan, "Modelling of scara robot dynamics by using neural network" Journal of Engineer and Machine, Volume: 46 Number: 550, Ankara 2005.

3. B. Roth, "Performance evolution of manipulators from a kinematic view point" NBS, Special Publication, pp.39-61, 1975

4. Y.C. Tsa, and A.H. Soni, "Accessible region and synthesis of robot arms" ASME I., Mechanical Design, Pp.803-811, 1981.

5. C.C.D. Lin and F. Freudens Tein, "Optimization of the workspace of a three-link turning–pair connected robot arm" International Journal of Robotic Research, Vol.5, pp.104-111, 1986.

6. S. Timoshenko and D.H. Young, "Engineering Mechanic" Publisher of Civil Engineering Faculty of İTÜ. İstanbul 1975.

7. A.S. Kara, "Mechanic Problems of Engineering Analyzed" Publisher of Güven, Ankara 1974.

8. F. Yücel, “Mechanic” Publisher of Ankara Üniversity, Publisher No: 273 Course Book, No: 95, Ankara 1966.

9. N.C. Braga, “Robotic mecatronic and artificial intelligence” Publisher of Bileşim, ISBN.9752711405, İstanbul 2005.

10. S. Kücük and Z. Bingül, “Workspace optimization of fundamental robot manipulators” IEEE 12th Mediterranean Conference on Control and Automation, Kuşadası, TURKEY.2004.

11. R.A. Kepner, R. Bainer and E.I. Barger, “Principles of Farm Machinery” Third Edition Avi Publishing Company, Inc. Westport, Connecticut, 1980.

Research on Calibration Reading Technology of High-Precision Meter

Zhigang Ning nzg0928@163.com
College of Electrical Engineering
University of South China
Hengyang,421001,China

Xueyu Gong gongxy@nhu.edu.cn
College of Electrical Engineering
University of South China
Hengyang,421001,China

Lihong Zhao zhaolh@gmail.com
College of Electrical Engineering
University of South China
Hengyang,421001,China

Changhong Shan shanch801@126.com
College of Electrical Engineering
University of South China
Hengyang,421001,China

Abstract

The paper proposes a way to achieve camera positioning tasks by 2D visual servoing. By observing both the camera and the features of meter reading, the camera is able to be positioned with an accuracy in hand-eye calibration. The calibration reading method is used to recognize high-precision meter reading.The paper mainly includes three parts. Firstly, the geometrical model of parallax formation is constructed and the importing error is analyzed. Secondly, according to the analysis of importing error, the calibration reading technology of high-precision meter and the experimental platform of calibration reading technology are designed. Finally, the experiment on the calibration reading technology is researched. The experimental results show the method is applicable to automatic recognition of high-precision meter.

Keywords: Calibration Reading Technology,High-Precision Meter,Camera Lenses Locating, Importing Error.

1. INTRODUCTION

Although many digital meters have output ports which can directly connect with computer digital output ports, it is difficult for some practical application to operate automatically and recognize meter reading with person's eye. In addition, sampling meter reading in some running systems or at some dangerous scenes is needed. Automatization and communication of these systems need improving.Intelligent examination method based on machine vision is a fundamental way to improve conventional examination method, which carries machine vision and artificial intelligence in meter detecting process. The method has eliminated personal error of labour examination and

improved examination precision and speed. The method is a new attempt of automatic technology applying to industrial production and examination process.
Industrial development and multi-subject cross-research need all sorts of examination meters. Because of output ports of different sorts of digital meters produced by different corporation and their communication agreements, it is a great workload that output ports are connected by all sorts of communication agreements. It isn't immediately realized that all kinds of meters with or without digital output ports are constituted an integrated and automatic examination system. Owing to above mentioned reasons, it is practically valuable that meter digital reading is photographed and recognized.
Dial meters with simple structure, easy use and low price are widely used to measure electrical current, distance, water, gas, etc. The precision level of recognition system of meter reading of dial meter is under 1.0 at the present time, while high-precision dial meter is not widely researched[1]. The paper adopts calibration reading technology to recognize meter reading of high-precision dial meter.The first stage of our research is focused on camera locating. Calibration reading technology is used to calibrate camera position, which makes optical center of camera lens locating in the permissible error area[2-4].
The paper is organized as follows. Section two discusses some of the relevant visual servoing positioning literature. The geometrical model of parallax formation is constructed and the importing error is analyzed in Section three.Section four describes the calibration reading technology of high-precision meter. The experiment on the calibration reading technology is shown in Section five.The paper ends with conclusion.

2. RELATED WORK

Traditional method of sensor-guided fine-positioning is based on hand-eye calibration. Hand-eye calibration is a process used in the field of robotics to determine the orientation of a camera in relation to the recognition of meter reading of high-precision dial meter. Only focusing on vision-based positioning relative to a static(unmoving) target, it can be argued that the basic principles for implementing visual feedback are well understood by now[5-6].With dynamic visual features, a positioning task consisting of moving the camera to the parallel position of a planar object is achieved[7]. A robot arm is used to locate a camera in known poses relative to an observed object [8].
2D visual servoing is based on using features directly calculated from the images which are used as input in the control scheme. Former work started using image points which is still one of the most popular primitivenesses today[5,9-10]. Other 2D primitivenesses have been modelled on straight line[5,11], segments, circles, ellipses, cylinders and spheres[5,12]. Some other work tends to combine different visual features in a unique control scheme. Point coordinates, area enclosed by points and angle between segments are used to improve the performance of the system[13]. Imaged-based visual servoing is traditionally robust against modelling errors of system. Since controlling is made in the image space, it is easier to design strategies to avoid the image features going out the image bounds[13-14]. Hybrid visual servoing approach combines 2D with 3D features. In case of knowing the model of the object, classic pose recovering algorithms can be used to estimate some 3D features as in position-based visual servoing. A lot of visual servoing approaches have been probed when the desired image is known. Some of them are based on recovering the partial pose between the camera and the object from the desired image and the current image[15-16].

3. ANALYSIS OF IMPORTING ERROR

The camera position greatly influences meter reading. Figure 1 is the stereogram of optical center of camera lens, meter pointer and scale. The plane Γ_1 is scale plane, and arc cd denotes the segment of scale line of dial meter on the plane Γ_1. The plane Γ_2 is pointer plane, and the line op denotes meter pointer on the plane Γ_2. The point o denotes rotary axis of meter pointer, and the point p denotes the tip of meter pointer. The plane Γ_1 and the plane Γ_2 are parallel to each other. The plane Γ_3 including meter pointer op is the vertical plane of pointer plane Γ_2. The point o' is an

optional point over the point o. The point o'' is the projection of the point o on the plane Γ_1. The point p'' is the projection of the point p on the plane Γ_1. The line $o''p''$ is the projection of meter pointer op on the plane Γ_1. The point p'' is on scale arc cd. The meter reading which the point p'' denotes is the accurate reading of meter without any parallax. The point f is an optional point over the line op, which is on the plane Γ_3. The point b' is an optional point above the line op, which is not located on the plane Γ_3. So the point b' is not located on the line $o'o''$. The line $o'b'$ and the plane Γ_2 are parallel to each other. According to the principle of parallax formation, reading parallax of meter is researched when optical center of camera lens is located at the point b', the point f and the point o' respectively. When optical center of camera lens is located at the point b', the line $b'p$ and the scale plane Γ_1 intersect at the point n, and the line $o''n$ and the scale arc cd intersect at the point j. The arc jp'' denotes reading parallax of meter. The line fp and the scale plane Γ_1 intersect at the point a. Because the intersecting point a must locate on the extended line $o''p''$, reading parallax of meter is zero when optical center of camera lens is located at the point f. The line $o'p$ and the scale plane Γ_1 intersect at the point m. Because the intersecting point m must locate on the extended line $o''p''$, reading parallax of meter is zero when optical center of camera lens is located at the point o' on the plane Γ_3. According to above mentioned analysis,when optical center of camera lens is located at any optional point over rotary axis of meter pointer or the line op on the plane Γ_3, which is the vertical plane of the plane Γ_1 and includes meter pointer op, reading parallaxes of meter don't exist.

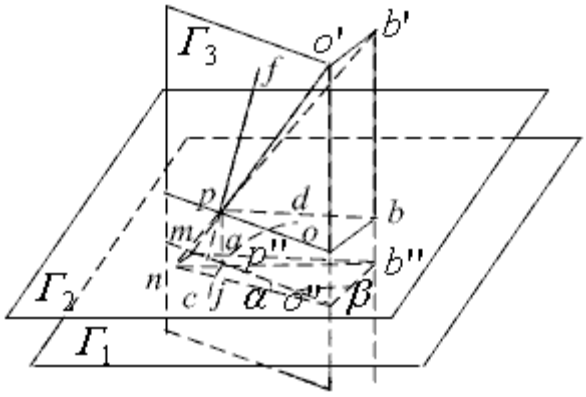

FIGURE 1: Stereogram of Optical Center of Camera Lens, Meter Pointer and Scale

The point b is the projection of the point b' on the pointer plane Γ_2. The point b'' is the projection of the point b' on the scale plane Γ_1. $o'b' \parallel ob \parallel o''b'' \perp mn$, $op \perp mo''$, $\perp mnp \perp \perp o'b'p$, $\perp o'po \perp \perp o'mo''$, $\frac{|mn|}{|o'b'|}=\frac{|mp|}{|o'p|}=\frac{|oo''|}{|oo'|}$, $\frac{|mo''|}{|op|}=\frac{|o'o''|}{|oo'|}$. So, $|mn|=\frac{|oo''|}{|oo'|}\times|o'b'|$, $|mo''|=\frac{|o'o''|}{|oo'|}\times|op|$. $\angle pob$ is the angle between the line ob and the pointer line op. If the pointer line op is rotated around the point o, the size of angle $\angle pob$ will change. $\angle mo''b''=\angle pob$, $\angle no''m=\alpha$, $\angle mo''b''=\beta$, so $\angle nmo''=\beta$. In the triangle $o''mn$, the following formulation is concluded on the foundation of law of sines:

$$\frac{|mn|}{\sin\alpha}=\frac{|mo''|}{\sin(180°-\alpha-\beta)}$$

By calculating, $\alpha=arcctg\left[\frac{(|oo''|+|oo'|)\times|op|}{|oo''|\times|o'b'|}\times\csc\beta-ctg\beta\right]$. The length of arc jp'' corresponding to reading parallax of meter is as follows :

$$err=\left|o''\,p''\right|\times\alpha=\left|op\right|\times\alpha=\left|op\right|\times arcctg\left[\frac{(\left|oo''\right|+\left|oo'\right|)\times\left|op\right|}{\left|oo''\right|\times\left|o'b'\right|}\times\csc\beta-ctg\beta\right] \qquad (1)$$

where, the degree of angle β ranges from - 180° to 180°. When camera lens lies on the right side of the vertical plane of pointer plane and scale plane, the projection of meter pointer lies on the left side of accurate reading of meter pointer, and meter reading is less than the accurate reading. The angle β is defined as a negative angle, and the reading parallax is defined as a negative reading parallax. When camera lens lies on the left side of the vertical plane of pointer plane and scale plane, the projection of meter pointer lies on the right side of accurate reading of meter pointer, and meter reading is bigger than the accurate reading. The angle β is defined as a positive angle, and the reading parallax is defined as a positive reading parallax. $|oo''|$ is the distance between the pointer plane Γ_2 and the scale plane Γ_1 .$|oo'|$ is the upright distance between the point o' and the pointer plane Γ_2 . $|o'b'|$ is the upright distance between the point b' and the line $o'o''$. $|op|$ is defined as the length of meter pointer. The tolerant error of 0.5 precision level milliammeter is 5‰, so the maximum of absolute permission error of scale is 0.07cm(5‰ ×100×0.14).If $|oo''|$=0.2cm,$|op|$=8cm,β,$|oo'|$ and $|o'b'|$ are three groups of different data respectively, all of importing errors are listed in Table 1.According to all data of Table 1, the maximal importing error is 0.019698 cm, and the percentage of maximal importing error to maximal scale permission absolute error is 28.14%. The big importing error increases reading parallax of meter undoubtedly. The higher the precision level is, the bigger the permission error is. So automatic recognition methods of high-precision meter need to be researched. The calibration technology of high-precision meter is researched in the paper. If optical center of camera lens is located at a point over rotary axis, the importing error doesn't exist.

err(cm) \ β / oo'	$\beta=60°$			$\beta=90°$			$\beta=135°$		
	$\left\|o'b'\right\|=0.5$ cm	1cm	1.5cm	0.5cm	1cm	1.5cm	0.5cm	1cm	1.5cm
$\left\|oo'\right\|=15$ cm	0.005698	0.011403	0.017101	0.006601	0.013202	0.019698	0.005499	0.009303	0.013902
$\left\|oo'\right\|=20$ cm	0.004298	0.008603	0.012901	0.004998	0.009898	0.014903	0.0035	0.007	0.0105
$\left\|oo'\right\|=25$ cm	0.003206	0.006902	0.010297	0.003997	0.007903	0.0119	0.0028	0.0056	0.0084

TABLE 1: Importing Error Calculating

4. CALIBRATION READING TECHNOLOGY

The calibration technology of camera is the key technology of precision measure in the computer vision field. Measure error of high-precision meter must be small, and the parallax of meter reading has a great influence on measure precision. In order to obtain the corresponding relative position between a special point and relevant image point, imaging system must be calibrated. According to the analysis of importing error, when optical center of camera lens is located at a point over rotary axis or meter pointer, reading parallax of meter doesn't exist. The process of calibration technology is based on the principle of parallax formation. When meter pointer points at zero scale and the maximal scale respectively, images of zero scale and maximal scale are photographed respectively. Then meter images of zero scale and maximal scale are recognized respectively. If optical center of camera lens is located at a point over rotary axis, camera or meter doesn't need to be moved.Otherwise, the relative position of camera and meter needs to be adjusted until optical center of camera lens is located at a point over rotary axis.

Computer test equipment system 1000(CTES-1000) is the experimental platform, which includes X-Y reference frame table, camera,computer, 0.5 precision level milliammeter, direct current power, resistance box and lamp-house. The X-Y reference frame table is controlled by X direction stepping motor and Y direction stepping motor. The high-precision meter is placed on the X-Y reference frame table. The orientation precision of X-Y axis is 0.005mm. Exprimental equipment is depicted in Figure 2.

FIGURE 2: Experimental Equipment

The algorithmic process of calibration reading technology is as follows:
 The high-precision meter is placed on X-Y reference frame table.
 When the meter is not electrified, meter pointer should point at zero scale. If meter pointer does not point at zero scale, adjusting zero device works by hand until meter pointer points at zero scale as depicted in Figure 3(a),which is confirmed by manual recognition method of simple eye.
 The meter image is photographed and recognized. If recognition result of meter image is zero,optical center of camera lens is deemed to be located at a point over rotary axis.Then the process is executed.
 If the recognition result of meter image isn't zero, X-Y reference frame table is moved and the meter image is photographed and recognized repeatedly, till the recognition result of meter image is zero.
 Standard power is electrified and controlled till meter pointer points at the maximal scale as depicted in Figure 3(b), which is confirmed by manual recognition method of simple eye.
 The meter image is photographed and recognized. If the recognition result of meter image is the maximum value of meter scale, optical center of camera lens must be located at a point over rotary axis and the calibration process is finished.
 If the recognition result of meter image isn't the maximum value of meter scale, X-Y reference frame table is moved in order to make optical center of camera lens moving along meter pointer direction and the meter image is photographed and recognized repeatedly, till the recognition result of meter image is the maximum value of meter scale. The calibration process is finished.
Meter images of pointing at different scales are depicted in Figure 3 as follows:

(a) Pointing at the Zero Scale (b) Pointing at the Maximal Scale

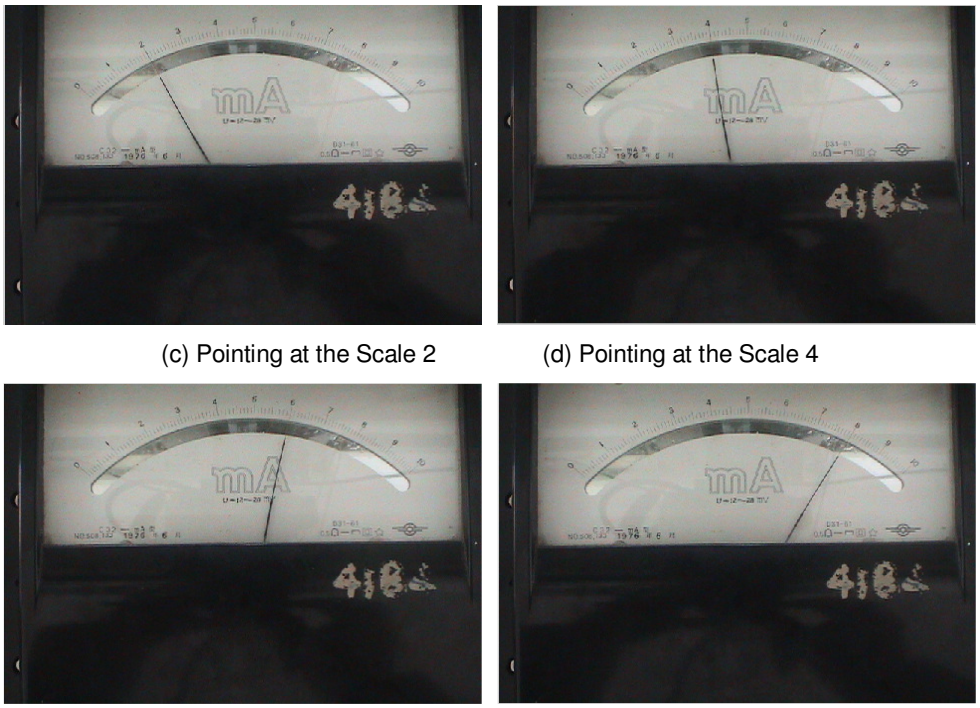

(c) Pointing at the Scale 2 (d) Pointing at the Scale 4

(e) Pointing at the Scale 6 (f) Pointing at the Scale 8

FIGURE 3: Meter Images of Pointing at Different Scales

5. EXPERIMENTAL RESULTS

The measurement range of milliammeter is between the current 0 mA and 50mA, and calibration reading technology is used to recognize the reading of milliammeter. Firstly meter pointer is conformed to point at the scale 0, the scale 2, the scale 4, the scale 6, the scale 8 and the scale 10 by manual recognition method of simple eye respectively. The scale 0, the scale 2, the scale 4, the scale 6, the scale 8 and the scale 10 correspond with 0mA,10mA,20mA,30mA,40 mA and 50mA respectively. Secondly meter image is photographed,when meter pointer points at the scale 0, the scale 2, the scale 4, the scale 6, the scale 8 and the scale 10 respectively, as depicted in Figure 3(a),(c),(d),(e),(f) and (b). Finally different meter images are recognized respectively. All recognition results are listed in Table 2.

Practical scale(mA)	0	10	20	30	40	50
Recognition result(mA)	0.002312	9.996288	20.006673	29.997416	40.001856	49.998483
Absolute error(mA)	0.002312	0.003712	0. 006673	0.002584	0.001856	0.001517

TABLE 2: Recognition Results

According to all data of Table 2, the maximum of meter reading parallax is 0.006673 cm, which is less than 0.007 cm(1 / 10×5‰×100×0.14). Because the maximum of parallax of meter reading is less than one tenth of the maximum of absolute permission error of scale, system error can be neglected.

The distance between camera lens and pointer plane ranges from 18 cm to 20cm, where meter image which includes all meter scales can be photographed. When the rotary center of meter is used as the center of circle, and the length of radius $|o'b'|$ is 0.1 cm, 0.2 cm, 0.3 cm, 0.4cm, 0.5 cm and 0.6 cm respectively, and the length of $|oo'|$ is 18 cm, 18.5 cm, 19 cm, 19.5 cm and 20 cm respectively, and β equals to 90° and - 90° respectively, maximal parallaxes of these zones can be calculated according to the formulation (1). All maximal parallaxes are listed in Table 3. The maximum of meter reading parallax is 0.006593 cm from all data of Table 3, which is less than 0.007 cm. Because the maximum of parallax of meter reading is less than one tenth of the

maximum of absolute permission error of scale, system error can be neglected. When optical center of camera lens is located over the circle zone where the rotary center of meter is used as the center of circle and the length of radius is 0.6 cm, reading parallax of 0.5 level precision meter is less than 0.007 cm, which can be neglected. The absolute error of each recognition result is less than 0.007 cm, which is within the range of permission error. So calibration reading technology is a feasible recognition method of high-precision meter in the paper.

$err_{\max}$(cm) oo' / $o'b'$	18 cm	18.5 cm	19 cm	19.5 cm	20 cm
0.1cm	0.001099	0.001070	0.001042	0.001015	0.000990
0.2 cm	0.002198	0.002139	0.002083	0.002030	0.001980
0.3 cm	0.003297	0.003209	0.003125	0.003046	0.002970
0.4 cm	0.004396	0.004278	0.004167	0.004061	0.003960
0.5 cm	0.005495	0.005348	0.005208	0.005076	0.004950
0.6 cm	0.006593	0.006417	0.006250	0.006091	0.005941

TABLE 3: $|o'b'|$ to Satisfy Parallax Permission Value

6. CONCLUSION

The automatic recognition method of high-precision meter can eliminate subjective error of manual recognition method, and improve the automation of measure. Calibration reading technology is a method of easy operation and realization, which is a good recognition method of high-precision meter.

7. ACKNOWLEDGMENT

The research work described in the paper was fully supported by a grant from the Natural Science Foundation of Education Department of Hunan province (Project No.08C751) and a grant from Doctor Startup Foundation of University of South China (Project No.2007XQD23).

8. REFERENCES

1. Zhigang Ning. *"Research on key technologies of meter image recognition"*.PhD Thesis, Guangdong University of Technology ,Guangzhou,China,June,2007.(In Chinese)

2. Jian Zhou,Hong Zhao,Feng Tian. *"Non-contact type photoelectric system for measuring displacement of rigid body"*.Opto-Electronic Engineering, 24(6):60-66,1997. (In Chinese)

3. Ying Zha,Tiegen Liu,Dong Du. *"Application of image recognition in automatic recognition system for part assembling"*.Computer Engineering,32(10):178-179,185,2006, (In Chinese)

4. Jianfei Mao,Jing Zhu. *"Study on high accurate calibration of industrial robot vision positioning system"*.Robot, 26(2):139-144,2004. (In Chinese)

5. B.Espian,F.Chaumette,P.Rievs. *"A new approach to visual servoing in robotics"*.IEEE Transactions on Robot and Automation,8:313-326,1992.

6. J.Feddema,C.Lee,O.Mitchell. *"Weighted selection of image features for resolved rate visual feedback control"*.IEEE Transactions on Robot and Automation,7(2):31-47,1991.

7. A.Cretual,F.Chaumette. *"Positioning a camera parallel to a plane using dynamic visual servoing"*.Proceedings of IEEE/RSJ International Conference Intelligent Robots and Systems,IROS'97,Grenoble,France,pp.43-48,September,1997.

8. P.Wunsch,G.Hirzinger. *"Registration of CAD-models to images by iterative perspective matching"*.Proceedings of the 13th International Conference on Pattern Recognition,Vienna, Austria,pp.77-83,August,1996.

9. C.Collewet,F.Chaumette. *"Positioning a camera with respect to planar objects of unknown shape by coupling 2-D visual servoing and 3-D estimations".*IEEE Transactions on Robot and Automation, 3(18):322-333,2002.

10. G.D.Hager. *"A modular system for robust positioning using feedback from stereo vision"*,IEEE Transactions on Robot and Automation,13(4):582-595,1997.

11. E.Malis,J.J.Borrely,P.Rives. *"Instrinsics-free visual servoing with respect to straight lines".* Proceedings of IEEE/RSJ International Conference Intelligent Robots and Systems,Vol.1, Laussane,Switzerland,pp.384-389,September,2002.

12. E.Marchand,F.Chaumette. *"Active vision for complete scene reconstruction and exporation".*IEEE Transactions on Pattern Analysis and Machine Intelligence,21(1):65-72,1999.

13. P.I.Corke,S.A.Allotta. *"A new partitioned approach to imaged-based visual servo control".* IEEE Transactions on Robot and Automation,17(4):507-515,2001.

14. Y.Mezouar,F.Chaumette. *"Path planning for robust image-based control".* IEEE Transactions on Robot and Automation,18(4):534-549,2002.

15. E.Malis,F.Chaumette. *"Theoretical improvements in the stability and analysis of a new class of model-free visual methods".* IEEE Transactions on Robot and Automation,18(2):176-186,2002.

16. G.Morel,T.Leibezeit,J.Szewczyk,S.Boudet,J.Pot. *"Explicit incorporation of 2D constraints in vision-based control of robot manipulators".*International Symposiums on Experimental Robotics,Vol.150,LNCIS,pp.99-108,Sidney,Australia,2000.Springer Verlag.

Adaptive Control of a Robotic Arm Using Neural Networks Based Approach

Mahdi Vaezi m.vaezi7777@gmail.com
Faculty of Electrical & Computer Engineering
Science and Research Branch of Azad University
Tehran, Iran

Dr. Mohammad Ali Nekouie Manekoui@eetd.kntu.ac.ir
Faculty of Electrical & Computer Engineering
K. N. T. University of Technology
Tehran, Iran

Abstract

A new neural networks and time series prediction based method has been discussed to control the complex nonlinear multi variable robotic arm motion system in 3d environment without engaging the complicated and voluminous dynamic equations of robotic arms in controller design stage, the proposed method gives such compatibility to the manipulator that it could have significant changes in its dynamic properties, like getting mechanical loads, without need to change designs of the controller.

Keywords: Robotic Arm, Nonlinear Multivariable System, Neural Networks, NARMA-L2 Controller, Speed Trajectory.

1. INTRODUCTION

The modern nonlinear control theorem's failure in taming planets which suffer from problems like lack of certainty or unknown parameters in their modeling, complex or prolix regnant equations and etc are predictable sequent of this fact that all classical control theorems are based on the exact identification of systems. This has caused the domination of conventional control theories, like PID, over today's practical systems [16]. Common mechanical manipulators are vastly used systems which make an example of mentioned issue; in [16] and even in discrete form in [17] the famous sliding mode method has been utilized to control robotic manipulator with its dynamic equations which has caused to tremendous design and computational efforts, in [7] another common nonlinear control method ,feedback linearization, has been used for the purpose with similar results, more computationally voluminous adaptive control has been implied on such system in [10], even more recent approaches like neural networks has been used to adjust conventional PIDs in [10]&[3], even most recent neural networks based approaches like NARMA could be used only for single variable systems as mentioned in [1]and[11]; In this thesis after describing the relations over a three dimension robotic arm a new control strategy is introduced with aim of inflicting the reference input trajectory behavior on its wrist point movement .

2. METHODS

The applied controller is based on the NARMA (nonlinear autoregressive moving average) predictive theorem, the mathematical bases are explained in [6], the representation of dynamic discrete systems using state equations is well known as is represented in (1):

$$\begin{aligned} x(k+1) &= f[x(k), u(k)] \\ y(k) &= h[x(k)] \end{aligned} \quad (1)$$

The problems of control related to system (1) can be stated at various levels of generality. These include the cases when we have the following:

1) f and h are known, and the state is accessible.

2) f and h are unknown, but the state is accessible.

3) f and h are unknown, and only the input and output are accessible.

Of course the case 3 is hardest to handle because system identification and control must be carried out with only observing input and output signals, if a control method can be applied on this case the two sampler cases are easy to handle.

Relative degree: if

$$\begin{aligned} \frac{\partial(h \circ f_e^k \circ f(x,u))}{\partial u} &= 0 \quad 0 \le k \le n-2 \\ &\neq 0 \quad k = n-1 \end{aligned}$$

Where the middle term in left side of equation above is the k time iterated composition of f, then the dynamic system is said to have a related degree of n [14].

In discrete system since by definition the state x(k+n) depends to the input sequence $U_n(k) = [u(k), u(k+1), u(k+n-1)]$, and the same state sequence so the equation (2) can be obtained:

$$x(k+n) = g[x(k), x(k+1), \cdots, x(k+n-1), u(k), u(k+1), u(k+n-1)] \quad (2)$$

With respect to (1) the equation (3) could be obtained:

$$y(k+1) = F[y(k), y(k-1), \cdots, y(k-n+1), u(k), u(k-1), \cdots, u(k-n+1)] \quad (3)$$

The last equation is similar with the nonlinear ARMA predictive formula [3]. If one extends (3) around it's input vector with this term that u(k) is at small amplitude compare to the systems equilibrium state then (4) could be obtained:

$$y(k+1) = f_0[y(k),\cdots,y(k-n+1),u(k-1),\cdots,u(k-n+1)] + g_0[y(k),\cdots,y(k-n+1),u(k-1),\cdots,u(k-n+1)]u(k)$$

(4)

This theorem still is not suitable to devise a control method, with a little more approximation (5) is acquirable:

$$u(k+1) = \frac{y_r(k+1) - \mathrm{f}[y(k), \ldots, y(k-n+1), u(k), \ldots, u(k-n+1)]}{\mathrm{g}[y(k), \ldots, y(k-n+1), u(k), \ldots, u(k-n+1)]} \quad (5)$$

The last equation is known as NARMA-L2 equation and first described is [13], with authorizing a suitable training strategy for a block that contains two neural networks which must pattern f & g functions (this block will emulate the uncontrolled planet) and then rearranging this two networks to achieve (5) a neural network based adaptive controller block is acquirable; the well known multilayer perceptrone networks seems to fit perfectly for this objective since they have proved ability to map any kind of math function between their input and output.

3. THEORY

This thesis contains part of the research that have been accomplished through author's master of science level final project about to designing a "3d hand movement trajectory system by a robotic arm" which focused on controlling the robotic arm, first the specified robotic arm's properties must be explained; A three rotational joints robotic arm is considered with length of 40 cm for the first & 20 cm for the second and third links, this establishment of robotic arms is very common and is known as RRR or humanoid robotic arm (fig,1 & 2) and fits best to emulate human movements.

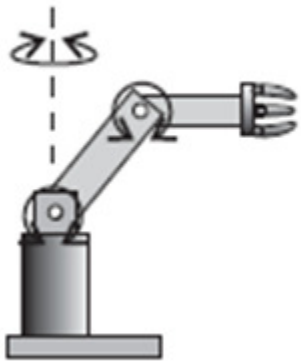

FIGURE 1: Common RRR Arm Topology.

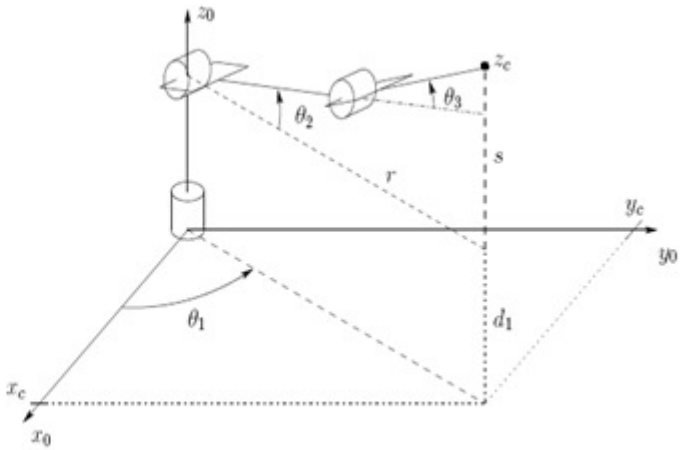

FIGURE 2: Detailed pattern.

using the standard Denavit-Hartenberg method [16] to analyze this robotic arm, the Jacobean matrix can be obtained from vector derivation of the direct kinematic matrix(6) , this kind of Jacobean matrix (7) gives the robot 's wrist point speed in three Cartesian directions in respect to its joints rotational speed(8), and the matrix's elements are three angelic functions of the joints angels. Also the invert Jacobean matrix does the inverse relation (9).

$$\begin{bmatrix} xe \\ ye \\ ze \end{bmatrix} = \begin{bmatrix} 0.2 * (\cos\theta 1 * \cos(\theta 2 + \theta 3) + \cos\theta 1 * \cos\theta 2) \\ 0.2 * (\sin\theta 1 * \cos(\theta 2 + \theta 3) + \sin\theta 1 * \cos\theta 2) \\ 0.2 * (\sin(\theta 2 + \theta 3) + \sin\theta 2 + 0.4 \end{bmatrix}$$

(6)

$$J = \begin{bmatrix} -\sin\theta 1 * \cos(\theta 2 + \theta 3) - \sin\theta 1 * \cos\theta 2 & -\cos\theta 1 * \sin(\theta 2 + \theta 3) - \cos\theta 1 * \sin\theta 2 & -\cos\theta 1 * \sin(\theta 2 + \theta 3) \\ \cos\theta 1 * \cos(\theta 2 + \theta 3) + \cos\theta 1 * \cos\theta 2 & -\sin\theta 1 * \sin(\theta 2 + \theta 3) - \sin\theta 1 * \sin\theta 2 & -\sin\theta 1 * \sin(\theta 2 + \theta 3) \\ 0 & \cos(\theta 2 + \theta 3) + \cos\theta 2 & \cos(\theta 2 + \theta 3) \end{bmatrix}$$

(7)

$$\mathrm{J} = \frac{\partial \mathrm{X}}{\partial \theta} \Rightarrow \frac{\mathrm{dX}}{\mathrm{dt}} = \mathrm{J}\frac{\mathrm{d}\theta}{\mathrm{dt}} \qquad (8)$$

$$\frac{\mathrm{d}\theta}{\mathrm{dt}} = \mathrm{J}^{-1}\frac{\mathrm{dX}}{\mathrm{dt}} \qquad (9)$$

These are the kinematic relations but there is more to be considered about robotic arms, equations (10) shows the general form of robotic arms dynamic equation.

$$D(\boldsymbol{q})\ddot{\boldsymbol{q}} + C(\boldsymbol{q}, \dot{\boldsymbol{q}})\dot{\boldsymbol{q}} + \boldsymbol{g}(\boldsymbol{q}) = \boldsymbol{\tau} \qquad (10)$$

In detailed form it is a extremely voluminous matrix equation with relative factors which explains the relation between actuators torque and respected joint's angel, rotational speed and acceleration through gravity, curiolis and torque terms. This equation is not utilized directly in this work so we postpone further explaining. The primary necessity for gaining propitious trajectory behavior is to design a suitable control diagram, with accent to preserve good precision in regulating an object's movement it seems adjusting its speed may bring better results than dealing directly with its position, it is guaranteed that the object will be in right position in right time if the ration of displacement with respect to time is accurate, so the control diagram in figure (3) is presented.

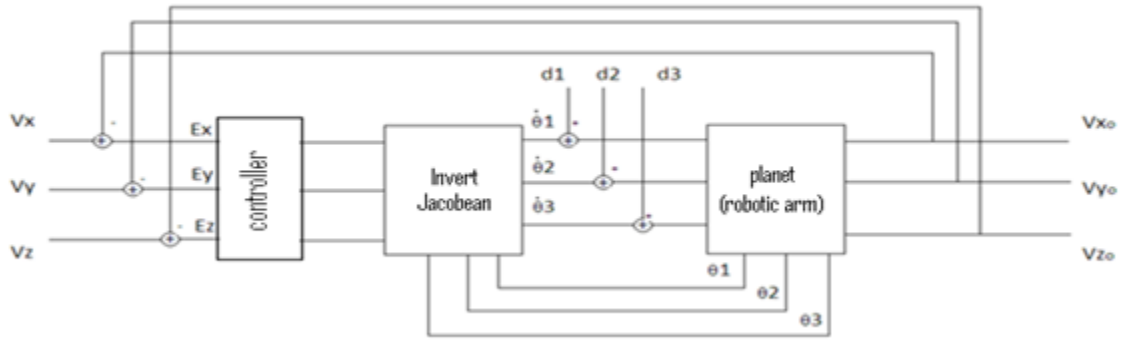

FIGURE 3: control diagram for the described system.

With the aim of problem statement the system state equations must be obtained, if x=θ is the 3×1 vector as the state variable and with neglecting controller block (k=1) the equation (11) can be obtained for the X axis, two others are similar.

$$\mathbf{Vx} = (\boldsymbol{Ux} + (\boldsymbol{J_{12}D_2} + \boldsymbol{J_{13}D_3}))/2 \quad (11)$$

This equation shows that in each axis the output is a direct function of input in addition of long and voluminous terms those are respectful of state variable and its derivatives. But where the disturbance input comes from? It has been shown in equation 11 that the robotic arm's dynamic relations cause a load torque in actuator, since every kind of actuators has a load-velocity profile with negative slope then the load torque (which is generated by dynamic effects) has the role of disturbance when the aim is to regulate the robot actuators velocity, for example the typical load-velocity profile of dc electrical actuator is shown in figure (4) [2]. The exact relations between input and output are acquirable but the state equations are very massive and this blocks the way to design any classical controller. It is also obvious that any control theorem that might be applied must be based on multi variable approach that doubles the required designing efforts and unguaranteed results; it seems the only remaining option is attending to implement the statistical approaches like neural networks based ones.

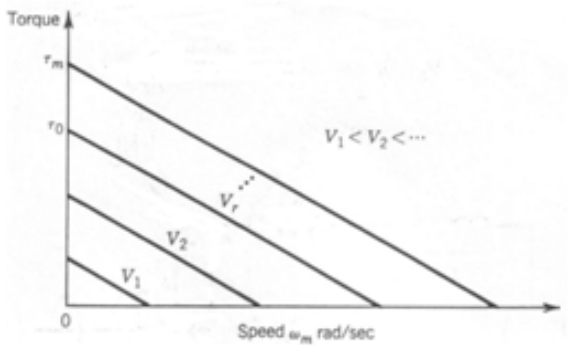

FIGURE 4: typical torque-velocity profile of dc servo actuators

Many researchers and authors have described methods like computing conventional PID compensator's factors using neural networks or genetic algorithms and it would be pointless to

focus on such methods. The intended method is based upon the paraphrased NARMA-L2 predictive method, to begin let's take another look to equation (5) as equation (12), this is also interesting that (12) is very similar to (11).

$$u(k+1) = \frac{y_r(k+1) - \mathrm{f}[y(k), \ldots, y(k-n+1), u(k), \ldots, u(k-n+1)]}{\mathrm{g}[y(k), \ldots, y(k-n+1), u(k), \ldots, u(k-n+1)]} \quad (12)$$

It is obvious that a propitious tracking behavior could be expected neutralizing this theorem when this is about a SISO system, but the current problem is with a multi input-output extremely nonlinear a voluminous system then how described NARMA-L2 approach might be useful here? The answer is acquirable with noting to two separate mathematical theorems:

Kolmogorov's existence theorem: "Every continuous N variable (input) function could be approximated using linear additions of nonlinear functions which are only relative with one of the variables". [8].

A multi layer percepteron neural network can emulate behavior of any type of mathematical function with unlimited discontinuous points [5].

So it could be said that a NARMA-L2 controller can emulate & control the described system's behavior if it contains two expedient networks and a suitable training strategy is applied, then for each input axis an individual controller block is needed; in order to train the networks perfectly for example networks related to controller X are connected to the planet model's adequate input and output while two other inputs have random pulse wave inputs in order to motivate all system modes (fig. 5).

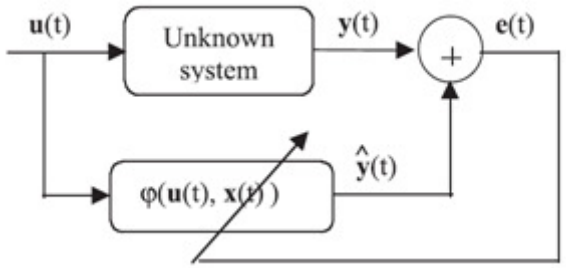

FIGURE 5: training strategy

In general three separated networks are used and each one has several delayed inputs and two out puts (parallel networks) to train and emulate f and g functions, in this case we don't know the exact state equations of the plant so the control method is called NARMA-L2 , if we knew the state equations this method would have been called neural based feedback linearization method, however figure 6 shows the networks general form in the simplest shape.

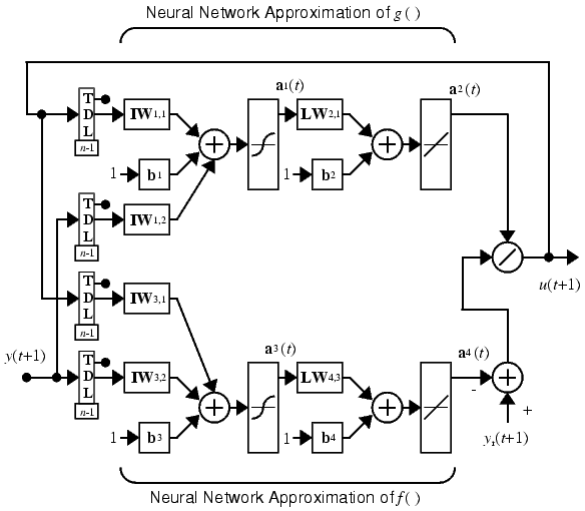

FIGURE 6: general formation of NARMA-L2 control made in MATLAB SIMULINK

There is only one neuron in hidden layer in fig. 6 but in practice more neurons are needed, usually between 10-13 hidden layer's neurons could handle the job , also number of delayed input is an important matter, since we don't know the degree of the plant's model (NARMA-L2 case) then number of delayed inputs must be obtained by examining in simulation, as described commonly robotic arms have very complicated and extensive ruling relations, in this works not less than 5 delayed inputs showed the suitable behavior. After getting the trained NARMA-L2 controller it must be connected to the plant, the general connection shape is shown in figure 7.

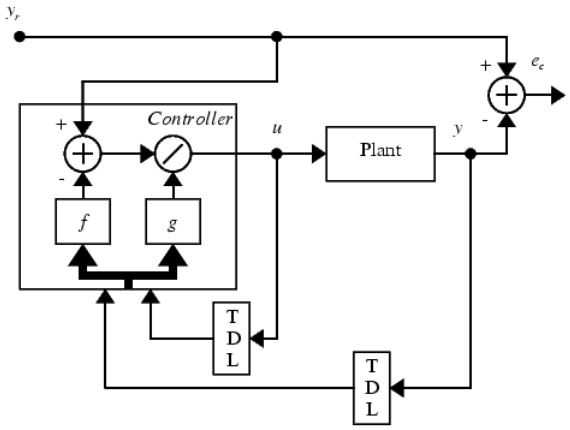

FIGURE 7: general shape for connecting the NARMA-L2 controller, error output could be useful for further experimentations.

And at last figure 8 shows the created formation of three NARMA-L2 controller in this work, note that in figure 3 there is feedback lines those are needed in classic control methods but in NARMA-L2 the conventional feedback is not used and the similar signal lines are needed to provide delayed inputs for the inside networks. The training performed using levenberg – marquardt method (trainlm), this presents a nonlinear algorithm for training multi layer perceptrones based on the Newton's method for minimizing functions which are consisted of linear sum of nonlinear functions squared form, this method has better performance and results

that many others but is profable only until several hundred neuron establishment of a network because of its high memory capacity requirement, the learning rule is shown in (13):

$$W(n+1) = W(n) - [J^T(n)J(n) + \mu I]^{-1} J^T(n)e(n) \tag{13}$$

Where μ is a factor which in small amount learning rule is Newton's formula with a hessian matrix and in larger amounts of μ this is gradient descent with small step size, since first form has faster and more accurate performance near a performance function's minimum point training's goal must be to reduce μ in every step' thus μ is always reduced and only in case of errors in crescent it steps up, and J is Jacobean matrix consisted of error's derivations with respect to weight factors variation shown in (14).

$$J(n) = \begin{bmatrix} \frac{\partial e_1(n)}{\partial w_1} & \frac{\partial e_1(n)}{\partial w_2} & \cdots & \frac{\partial e_1(n)}{\partial w_n} \\ \frac{\partial e_2(n)}{\partial w_1} & \frac{\partial e_2(n)}{\partial w_2} & \cdots & \frac{\partial e_2(n)}{\partial w_n} \\ \vdots & \vdots & \ddots & \vdots \\ \frac{\partial e_N(n)}{\partial w_1} & \frac{\partial e_N(n)}{\partial w_2} & \cdots & \frac{\partial e_N(n)}{\partial w_n} \end{bmatrix} \tag{14}$$

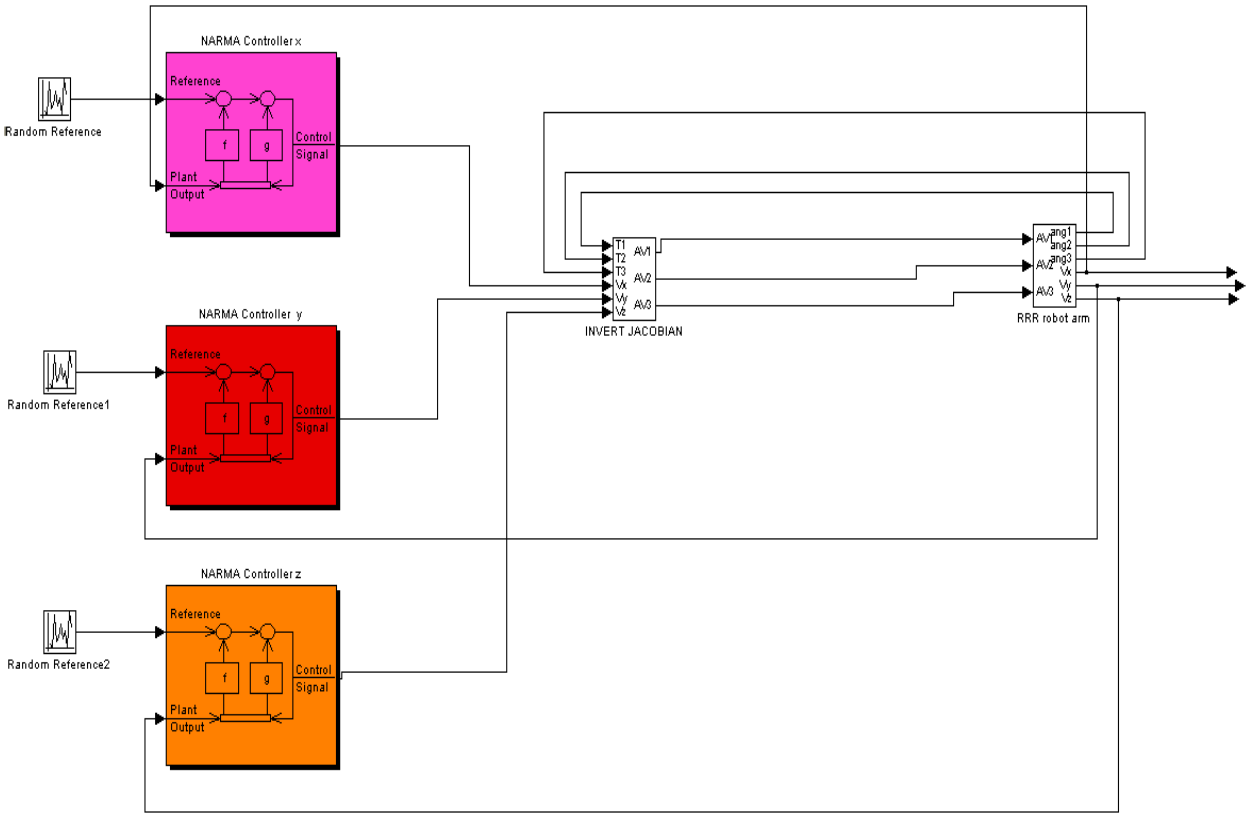

FIGURE 8: experimental formation of NARMA-L2 control of described three input-output robotic arm plant.

3. SIMULATION EXPERIMENTAL RESULTS

The whole system could be simulated in MATLAB SIMULINK, after making the planets model the three NARMA-L2 controllers trained executing the paraphrased strategy, the following figures are the three stage of networks training (training, testing and validating sets), figures 9 for NARMA-L2 controller X, 10 for Y & 11 for Z.

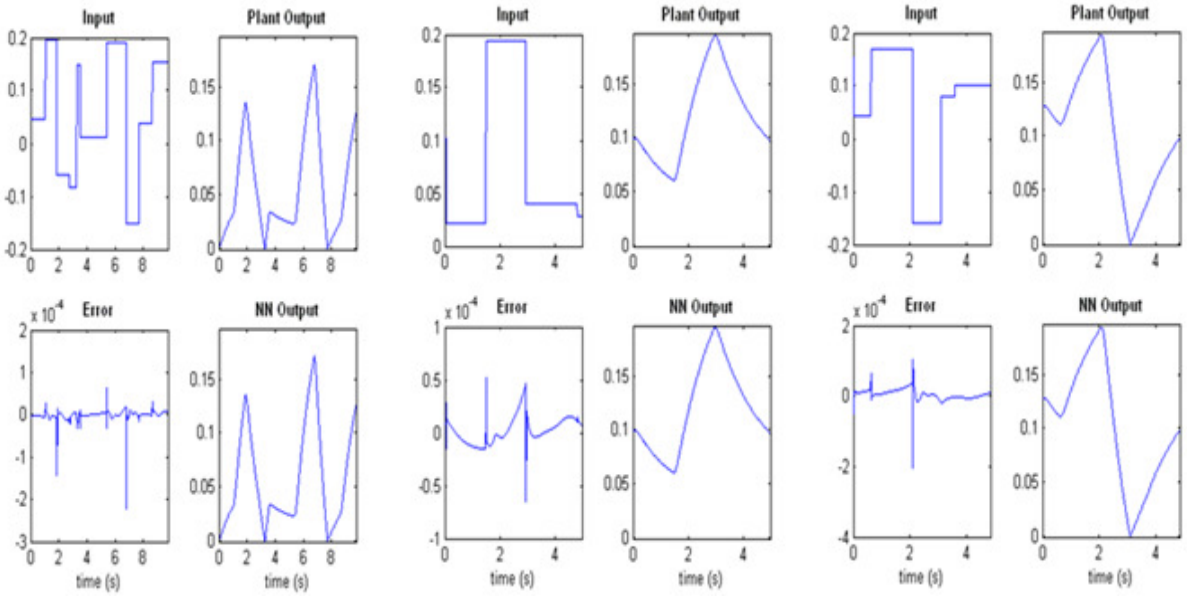

FIGURE 9: training, testing and validation sets for the NARMA-L2 controller in axis X, this figures also show the untamed plant's respond to puls inputs.

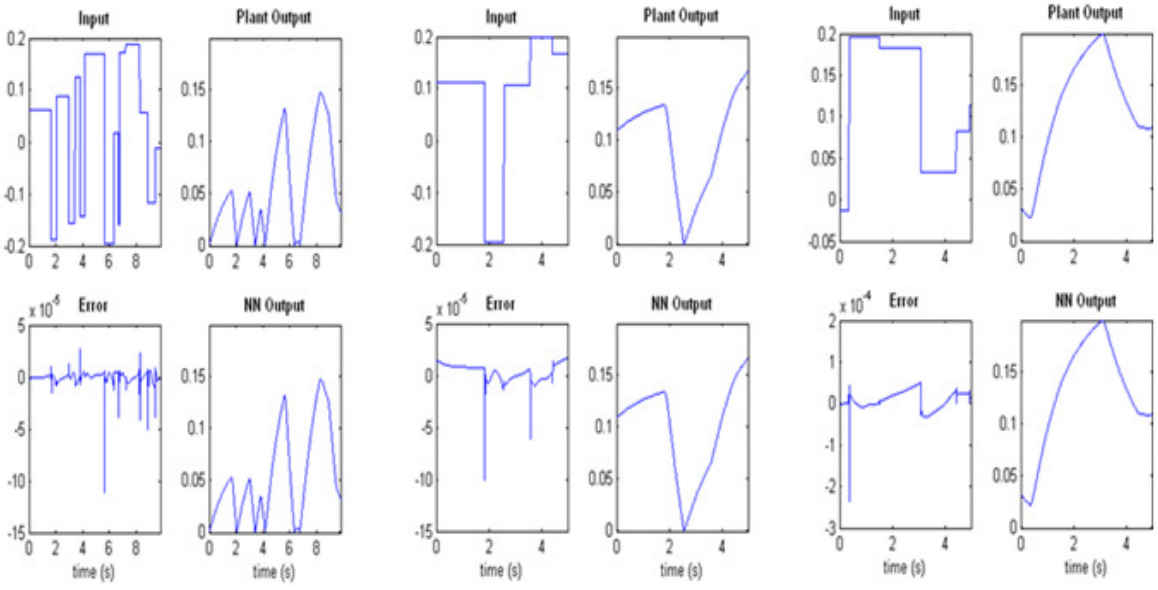

FIGURE 10: training, testing and validation sets for the NARMA-L2 controller in axis Y, this figures also show the untamed plant's respond to puls inputs.

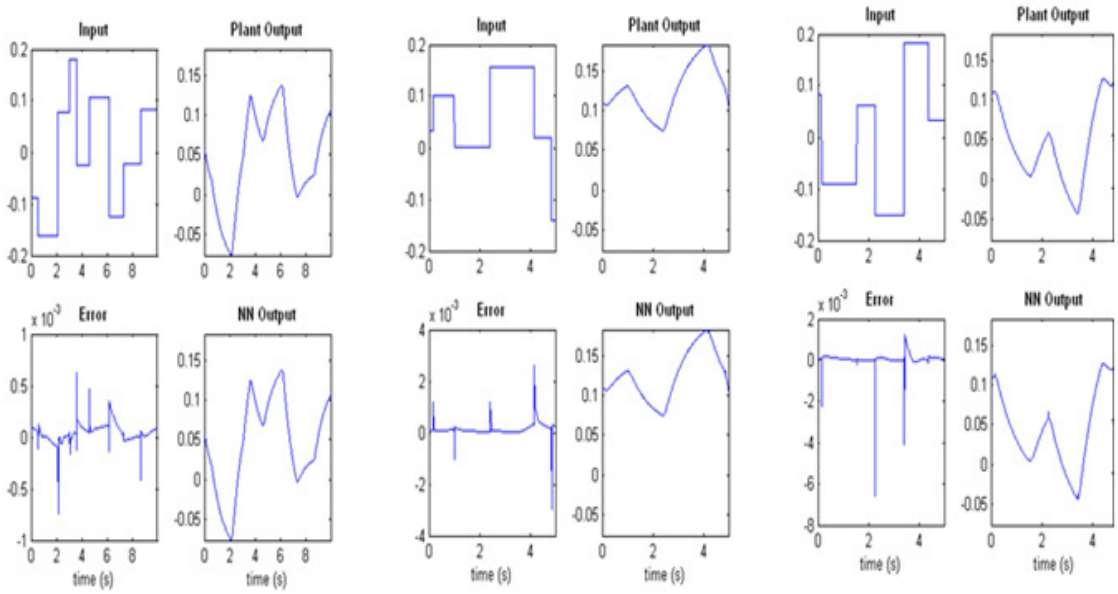

FIGURE 11: training, testing and validation sets for the NARMA-L2 controller in axis Z, this figures also show the untamed plant's respond to puls inputs.

After some retryings in training procedure a suitable reffrence tracking behaviore could be obtained, it seems that NARMA-L2 controller does the best about this system with 14 hidden layers and 5 delaied input-outputs; figue 12 shows the trajectory profile in X axis and the two other for Y and Z.

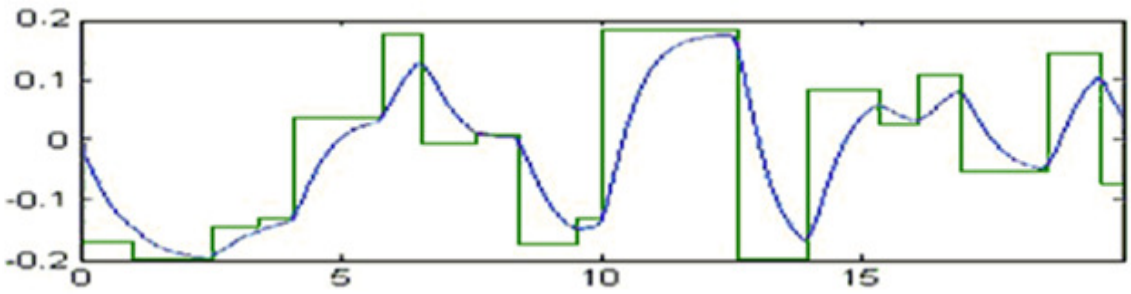

FIGURE 12: controled plant's refrence tracking profile in axis X neutralizing NARMA-L2 control method.

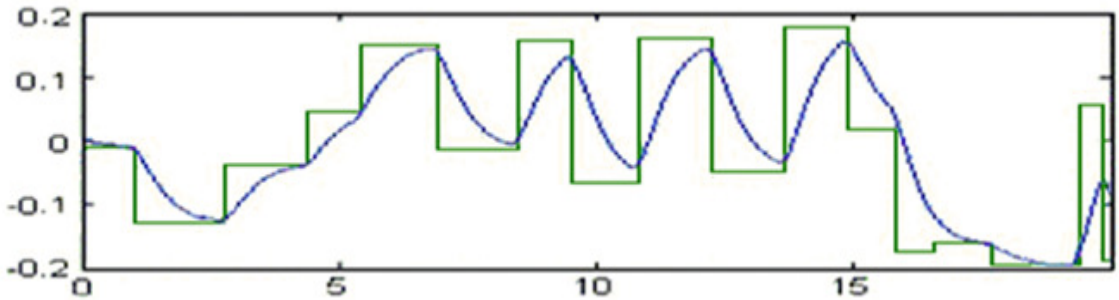

FIGURE 13: controled plant's refrence tracking profile in axis Y neutralizing NARMA-L2 control method.

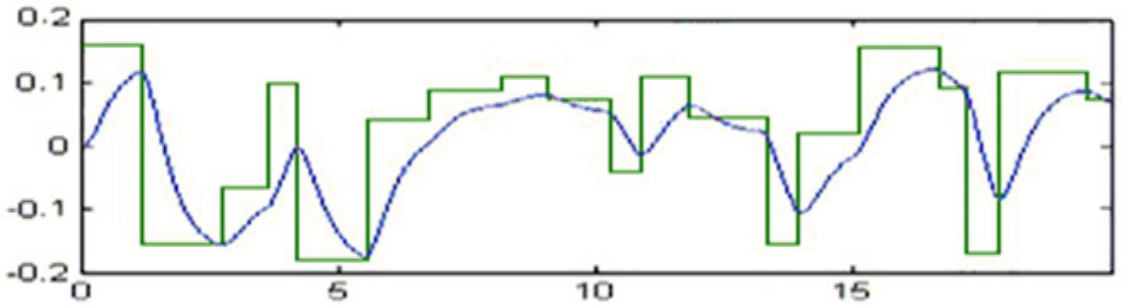

FIGURE 14: controled plant's refrence tracking profile in axis Z neutralizing NARMA-L2 control method.

4. CONCLUSION

This new approach for the robot control porpuse suffers from the extra ordiniary training properties, all neural networks based methods have a training phase but in this particular case training is a little more prolix and needs more efforts. There is also several concession point, like profable trajectory behaviore and not a very coplicated designing, then again it could be said that the proposed control strategy may eliminate the necessarily of complex driver boards for the actuator's control [12]; most importantly because all dynamic quandaries have the disturbance role in control loop but they could be included during the training procces, like manipulating a load with the robotic arm in addition of a gripper, the convinsing PWM shaped output provided by NARMA-L2 controlers for DC actuators are sufficient evidence for this claim. But after all it seems that the most important properties of this input trajectory system is that this control method has forced a similar output for step inputs in all manners, this is not guaranteed that a nonlinear system shows such behaviore (nonlinear systems respond is extremly related to their initial conditions, chaos theorem) but now with a suitable control method and training strategy it seems that the nonlinear multi input-output systems respond to step input similarily during simulation, now the way is clear to identify the whole system as three linear second degree systems and present a conventional PID controller for each input in order to further improvement in robotic arm's refrence trajectory profile.
Yet the advantages of this control methods should be counted as follow:

1- elimination of relativly expensive robot actuator's driver board's necessity.

2- the explained extremly nonlinear system has been seen showing a behaviore like simple identifiable linear system.

3- the whole control method should need less hardware equipments compare to those are necessary to establish complicated nonlineare controlers.

4- the utilized neural networks based control method has a discrete nature which is most desirable when it comes to implanting the system on digital chipsets.

5- while simulation some times errors accured when the robotic arm's configoration approach singulare configuration, but situations got handeled by reducing the simulation's time step, it seems the NARMA-L2 controlers can handle the conditions; since this control system is designed for input signal which is generated in wrist trajectory and hand operation stimulation (speed and

position in 3d) so in practice such situation should never accure becouse human arm's operation space is limited and it doesn't reach singular configuration which happen in arm's far reaches.

Further research and expansion outlines should be to investigate that if further changes in mechanical properties of system (like grasping an object) could be handles by adjusting a PID controler to whole now linearized system (or the training may be resumed),as the main fallback in neural networks based control methods is the fact that with any change in system trait obliges the training procedure repeated (yet it is worse in nonlinear controlers becouse whole design must be changed) , and to investigate how much training effort is required in practice.

5. REFFRENCES

[1] D.Beldekas. *"Comparative Control of A Nonlinear First Order Velocity System By A Neural Network NARMA Method".* Issn 1392 – 1215 Elektronika Ir Elektrotechnika.2004. Nr. 6(55):1-4, 2004.

[2] R.Bishop. *"Mechatronics",* Taylor & Francis Group, PP. 129-136 (2006).

[3] C.Cox. *"Modern Adaptive Control with Neural Networks".* International Conference on Neural Networks Information Processing, Iconip 96, Hong Kong, 1996.

[4] M.Haggan. *"neural networks design",* PWS publishing company, PP.391-399 (1996).

[5] S.Hawkins. *" Neural Networks",* Prentice Hall, PP. 130-170 (1999).

[6] Hen Yu, Hen. *"Handbook of Neural Network Signal Processing",* CRC Press, PP. 34-39, 42-71, 249-267 (2002).

[7] M.Koot. *"Identification And Control Of The RRR-Robot".* M.Sc thesis, Eindhoven University Of Technology,Serbia, 2001.

[8] R.Lippmann. *" An Introduction To Computing With Neural Nets".* IEEE ASSP Magazine: 4-22, 1987.

[9] L.Guoping. *"Variable Neural Networks for Adaptive Control Of Nonlinear Systems"* IEEE Transactions On Systems, Man, And Cybernetics—Part C: Applications And Reviews: 1-3, 1999.

[10] L.Marton. *"Robust-Adaptive Control of Nonlinear Single variable Mechatronic System".* PhD thesis, Budapest University of Technology And Economics, 2006.

[11] H. Mokri. *"Real Time Implementation of NARMA Control of a Single Link Manipulator".* American Journal Of Applied Sciences 5 (12): 1642-1649, 2008.

[12] G.Moleykutty. *"Speed Control of Separately Excited Dc Motor".* PhD Thesis, Multimedia University Melaka Campus, 75450 Melaka, Malaysia, 2008. [13] Narendra. *"Identification And Control Of Dynamical Systems Using Neural Networks".* IEEE Transaction of Neural Networks: 4-27, 1990.

[14] H.Nijmeijer. *"Nonlinear Dynamic Control Systems".* Springer, PP.130-160 (1990)

[15] Pandian, Shunmugham. *"Model-Based Sliding Mode Control of Underwater Robot Manipulators".* International Journal of Offshore and Polar Engineering (ISSN 1053-5381) Vol. 16, No. 3, September 2006: PP. 210–217, 2006.

[16] M.Spong. *"Robot Dynamic And Control",* Springer, PP: 61-83,99-153,175-193,231-300 (2004).

[17] G.Van Der Zalm. *"Discrete-Time Sliding Mode Control of the RRR-Robot"* PhD Thesis, Eindhoven University Of Technology, 2003.

Detecting Diagonal Activity to Quantify Harmonic Structure Preservation with Cochlear Implant Mapping

Sherif A. Omran sherif.omran@gmx.de
Mathematics and Natural science / Institute of Neuroinformatics / University of Zurich, 8057
Experimental Audiology Department / University Hospital of Zurich, 8091
Zurich, Switzerland

Abstract

Matrix multiplication is widely utilized in signal and image processing. In numerous cases, it may be considered faster than conventional algorithms. Images and sounds may be presented in a multi-dimensional matrix form. An application under study is detecting diagonal activities in matrices to quantify the amount of harmonic structure preservation of musical tones using different algorithms that may be employed in cochlear implant devices. In this paper, a new matrix called "Omran matrix" has been proposed. When it is post multiplied with another matrix, the first row of the output represents indices of fully active detected diagonals in its upper triangle. A preprocessing matrix manipulation might be mandatory. The results show that the proposed matrix is powerful in this application and illustrated higher grade of harmonic structure preservation of one algorithm used for cochlear implants with respect to other algorithms.

Keywords: Robotics, Cochlear Implant, Diagonal Detecting, Lines Detecting, Matrix, Harmonic Structure, Music.

1. INTRODUCTION

Cochlear implants (CIs) are devices aimed at restoring speech perception. The Nucleus cochlear implant uses a standard frequency to channel mapping algorithm that distorts harmonic structure of overtones in musical tones especially at low frequencies. Two new mapping algorithms based on semitone (Smt) mapping were developed and tested [1, 2]. These algorithms in addition to the standard mapping algorithm were used to process synthetic musical sounds and resynthesize them using a noise band vocoder acoustic model [3]. This paper aims at quantifying the degree these algorithms can reach in preserving the harmonic structure of overtones of musical tones. Sound signals are describable in three dimensions (intensity, frequency and time) and music is a complex sound that consists of tones. In general, tones have harmonically related partials [4]. Detecting active diagonals in matrices may be considered one way to detect harmonic structures in successive tones. The index of a detected diagonal in a frequency time matrix can represent the ratio between different overtones in such a case. Pattern recognition of objects inside matrices may be time consuming, but using the proposed Omran matrix (O'mat), matrix manipulation may be an easier approach. This paper is organized as follows:- Section 2 introduces a hypothesis and section 3 describes O'mat in details in addition to some examples in different special cases. Later, the algorithm is summarized in simple steps followed by a study using special acoustic signals, representing synthetic musical notes processed with the different algorithms; standard and semitone (Smt-MF and Smt-LF) mappings [1]. The output is preprocessed and is multiplied with O'mat. Section 4 is a proposed application for quantifying harmonic structure preservation using different music processing algorithms for CIs. Section 5 presents the results, where the following sections are discussion and conclusion.

2. HYPOTHESES

Preserving harmonic structure of music while being processed with a non-linear device, algorithm or a telecommunication system is expected to ameliorate music naturalness. Smt mapping which is one of the algorithms under study is expected to increase preservation of harmonic structure of overtones in CI devices because of its underlying nature.

3. METHOD

Definition: O'mat is a vertical rectangular or square matrix O[i,j] described by Equation 1. A matrix A is singular if the system Ax = 0 has non trifle solutions [5]. The vertical rectangle form of O'mat is invertible unless using the Moore-Penrose pseudo inverse. The first square B of the Moore-Penrose pseudo inverse of O'mat can be singular [6], where B matrix has dimensions equals to the rank of O'mat.

$$\text{Matrix } O[i,j] = \begin{cases} 0, & i=m,\ j=n \text{ for } i \neq j \text{ and } i \geq j \\ m-n+1, & i=m-n+1,\ j=c \text{ where } 1 \leq c \leq m-1 \text{ and } i \geq j \end{cases} \quad \text{Equation 1}$$

Each diagonal in the matrix is given a representative incrementing index number (see Figure 1).The first diagonal starts with index =1 and increments up to the main diagonal of the matrix. For appropriate recognition, each diagonal has to be fully active otherwise shifting the matrix one row upward and one column left or a matrix manipulation may be mandatory in a preprocessing phase. Lower triangles cannot be directly detected unless with matrix shifting or transposition.

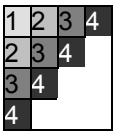

FIGURE 1: Diagonal indices of a matrix are shown in the same color. Each diagonal in the upper triangle of the matrix has a unique index number.

O'mat is a newly proposed matrix with zeros every where except the main diagonal of the lowest square as defined by Equation 1 and illustrated in Figure 2. All the values along the main diagonal increment by one and have their maximum which equals to the number of rows (i) at the lowest right corner. Figure 2 shows an example for a 4x4 (square) and 4x3 (vertical rectangle) O'mat. It illustrates two O'mats with 4 rows (i=4) (square and rectangular shapes).

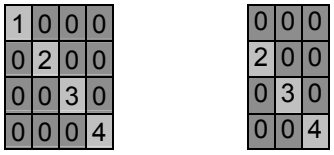

FIGURE 2: An example of a square (left) and a vertical rectangular (right) shape of O'mat with i=4. O'mat can not be horizontal by definition.

3.1 Proof

Assume an image B (4x4) with 2 diagonals active and the corresponding O'mat (4x4) matrix O

B=

0	a	b	0
c	d	0	0
e	0	0	0
0	0	0	0

O=

1	0	0	0
0	2	0	0
0	0	3	0
0	0	0	4

Result = B x O

=

0	2a	3b	0
1c	2d	0	0
1e	0	0	0
0	0	0	0

R(i,j) = B(i,j).O(j,j)

Assuming that the B image is binary (black=0 and white=1) and B(n,m) = 1 are elements in an active diagonal.

R(n,m)= 1. O(m,m) Equation 2

Equation 2 shows that the elements in the resulting matrix (R) that represent the active diagonals will not be dependent on the image, however the output will represent O'mat values in a decrementing arrangement. The following section has numerous examples in many special cases to illustrate the idea.

To understand the concept, let's start with a simple example for a non-singular O'mat and a binary image matrix image with four pixels. The lowest right element at i = m and j = n should be divided by the number of rows (i) in O'mat prior to being multiplied with O'mat. This is illustrated in the following examples:-

3.2 Example 1

Image x O'mat = Output

0	1	1	0
1	1	0	0
1	0	0	0
0	0	0	¼

x

1	0	0	0
0	2	0	0
0	0	3	0
0	0	0	4

=

0	2	3	0
1	2	0	0
1	0	0	0
0	0	0	0

EXAMPLE 1: To detect diagonal activities in an image using a non singular O'mat.

| Determinant (Output) | = 3! x 2! = 6

$$Weight = \prod_{1}^{n} output(1,n)! \text{ where } , output(1,n) \neq 0 \quad \text{Equation 3}$$

= 3! x 2! = 6

The weight value is calculated by multiplying all non zero elements in the first row of the output matrix as described by equation (3). In this example, the determinant of the output equals to its weight.

3.3 Example 2

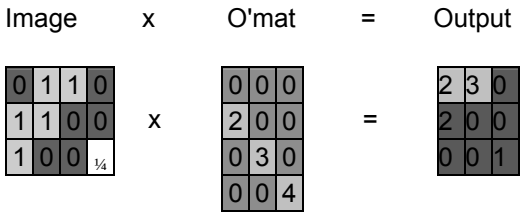

EXAMPLE 2: To detect diagonal activities in an image using O'mat, whose first square of its pseudo inverse is singular while the output is a non-singular square matrix.

$$Weight = \prod_{1}^{n} output(1,n)! \text{ where } , output(1,n) \neq 0$$

= 3! x 2! = 6

Both examples illustrated that the weight value is a factorial multiplication of the diagonal indices in the images that were fully active (see Figure 1).

3.4 Example 3

The following examples illustrate the case when the image is singular.

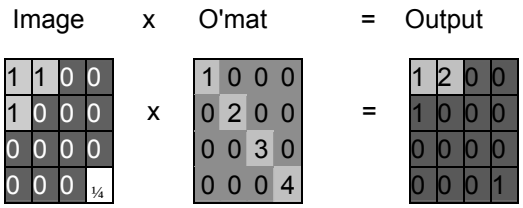

EXAMPLE 3: To detect diagonal activities in an image represented by a singular square matrix. One drawback of O'mat is inability to detect activity in diagonal with index =1.

| Determinant (Image) | = 0

$$Weight = \prod_{1}^{n} output(1,n)! \text{ where } , output(1,n) \neq 0$$

= 2! x 1! = 2

3.5 Example 4

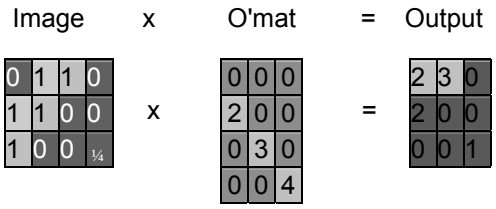

EXAMPLE 4: To detect diagonal activities in an image represented by a rectangular matrix having diagonal with index numbers 2 and 3 fully active using a rectangular O'mat.

$$Weight = \prod_{1}^{n} output(1,n)! \text{ where } , output(1,n) \neq 0$$

= 2! x 3! = 6

The weight value may be very complex especially in large matrices; it would practically exceed double precision length. To simplify the formula, an estimated weight function is proposed as in Equation 4:

$$\textit{Estimated Weight} = \sum_{1}^{n} 2^{output(1,n)} \qquad \text{Equation 4}$$

Steps to detect a diagonal activity:-

1 - Construct a zeros vertical rectangular or square matrix $_{(i,j)}$, where i≥j
2 - Fill the diagonal of the lowest square with decrementing numbers starting at element (i=n, j=n)
3 - Change the last (i,j) element in the image matrix into unity divided by n
4 - Post multiply O'mat with an image matrix that has a diagonal activity.
5- Check output diagonal values being decreasing by 1.
6 - Multiply the factorial of all non-zero elements in the first row of the output by each other to get the weight.
7- The indexes of the active diagonals exist in the first row of the output matrix.
8- Check the activity of the first elements (1,j) of the input image manually.

The matrix could be built with a simple Matlab script as shown in Figure 3.

```
function x=omran_matrix(i,j)
% Input : Required matrix dimension (i,j)
% Output: Omran Matrix
if nargin < 2,
    x=[];
    disp('please give matrix dimensions');
    return
end
if i<j,
    x=[];
    disp('Error: dimensions are not correct. Matrix can be vertical or square i>=j');
    return
end

x=zeros(i,j);
counter=1;
for q=i-j+1:i
    x(i,counter)=q;
    counter=counter+1;
end

end
```

FIGURE 3: A function to construct O'mat written in Matlab from Mathworks.

4. APPLICATION

Music is a complex sound consisting of tones which in turn, consists of fundamentals and overtones that generally have harmonic structure [7]. The majority of musical instruments have fundamental frequencies below 1 kHz [4]. Music is a sound that can be organized mainly in three elements (melody, rhythm and harmony) [8]. Melody is one of the important aspects of music [9], and is described as a sequence of individual tones that are perceived as a single entity [10]. Preserving the harmonic structure of individual tones is assumed to be necessary for preserving the melody perception.

One way to improve melody representation in CIs would be to ensure that the fundamental frequencies of adjacent tones on the musical scale are assigned to separate electrodes [1]. Such an approach involves mapping fundamental frequencies of musical tones to electrodes based on a semitone scale. The idea was initially investigated in a study by Kasturi and Loizou [11], using the 12 electrode Clarion CII (Advance Bionics) implant with a limited range of semitone frequencies. They concluded that semitone spacing improved melody recognition with CI recipients. Additionally, music could be enhanced by increasing the frequency representation. This may be possible using virtual channels (VCs) formed by stimulating two adjacent electrodes simultaneously with the same current level. Busby and Plant [12] reported that VCs invoked the perception of an intermediate pitch. VCs on an array of 22 electrodes would yield a total number of 43 channels, which would cover three and a half octaves with Smt mapping with one-semitone intervals between the characteristic frequencies of successive channels. A comparison between Std and Smt mapping with normal hearing and CI recipients showed a perceptual improvement in melody recognition [2]. In this paper, the amount of harmonic structure preservation is calculated quantitatively and relatively utilizing a special constructed sound signal that was processed with Std, Smt-MF and Smt-LF mappings and then re-synthesized with a noise band vocoder acoustic model for CI devices [3].

A sequence of 36 complex harmonic tones is prepared; each tone has the fundamental frequencies of piano note for a period of 100 msec with 4 overtones. The semitone mapping is claimed to preserve the harmonic structure of overtones as shown in Figure 4 and Figure 5 (22 and 43 channels respectively) where the ratio between the overtones with Smt mapping is almost constant; unlike with the Std mapping where there is a distortion of the harmonic structure at low frequencies. A Matlab program was developed for preprocessing before applying the O'mat algorithm. Harmonic structure preservation is demonstrated by a linear frequency to channel relationship, as can be seen for Smt-MF and SMT-LF for each of the partials. With the Std mapping, the linearity is seen only for the higher frequencies. At lower frequencies, the partials can not even be resolved. With Smt-MF components below 440 Hz are filtered out and with Smt-LF the high frequency partials greater than 1.51 kHz are filtered out (as indicated by arrows) [1].

a)

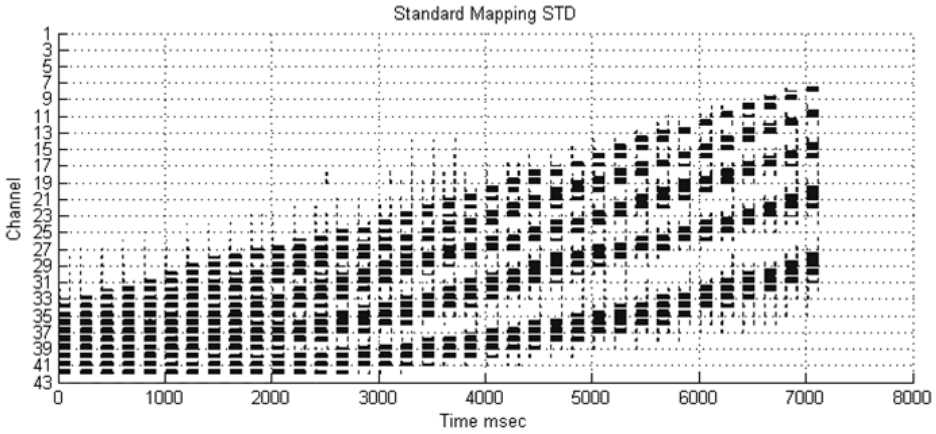

b)

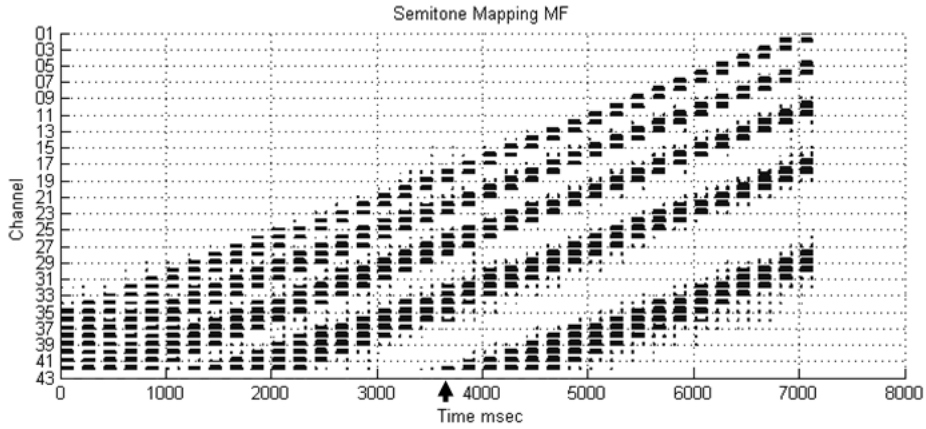

c)

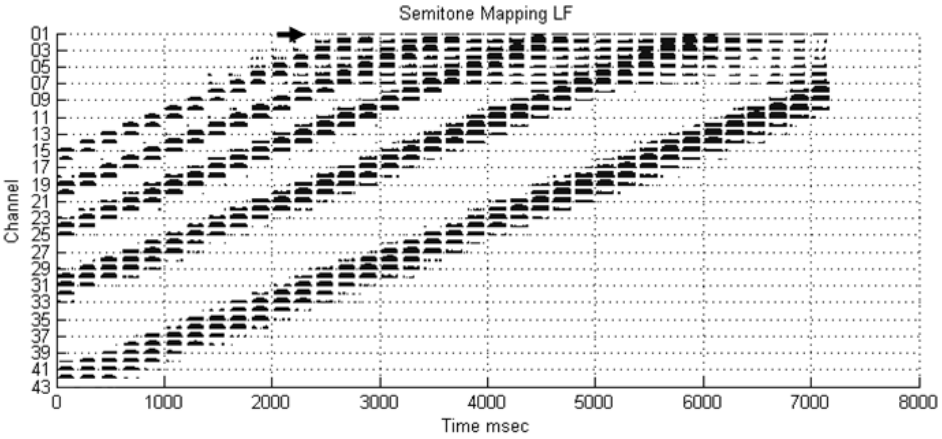

FIGURE 4: CTM outputs from the AMO for the Std (left), Smt-MF (middle) and Smt-LF (right) mapping using 43 channels.

a)

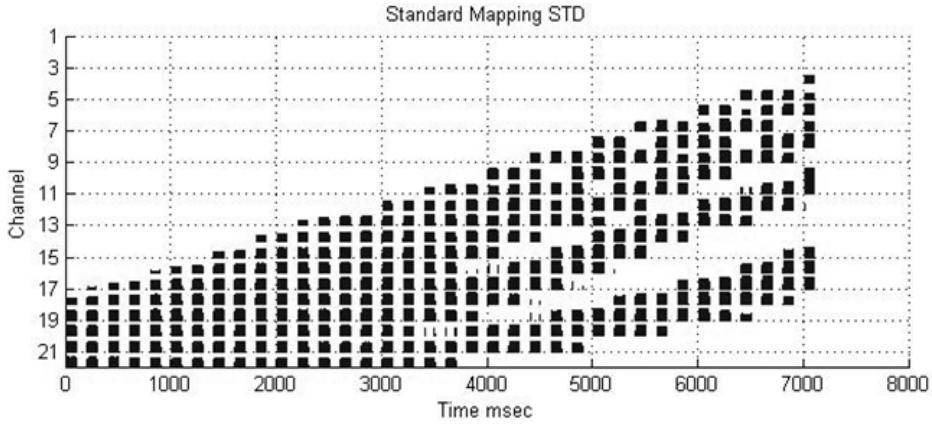

b)

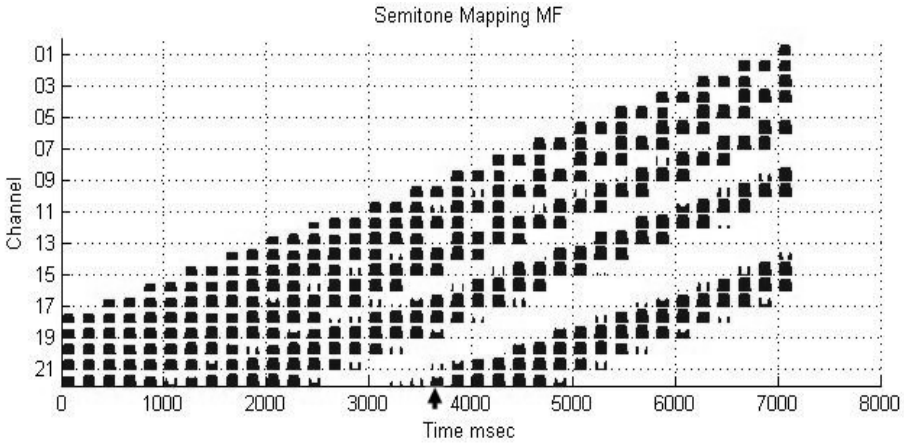

c)

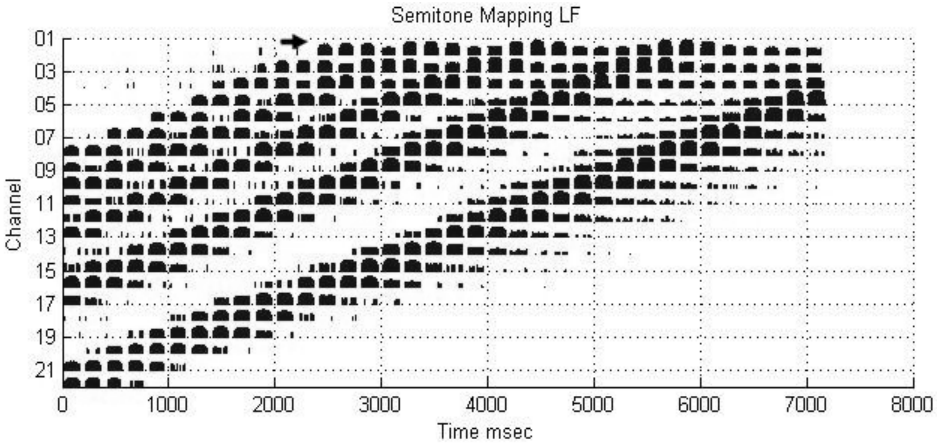

FIGURE 5: CTM outputs from the AMO for the Std (left), Smt-MF (middle) and Smt-LF (right) mapping using 22 channels.

5. RESULTS

Signals were preprocessed with an acoustic model [3] representing different algorithms for CIs using Std and Smt mappings with 43 and 22 channels [1, 2], The results are demonstrated in Figure 6 as a relative ratio of harmonic structure preservation with respect to Std mapping.

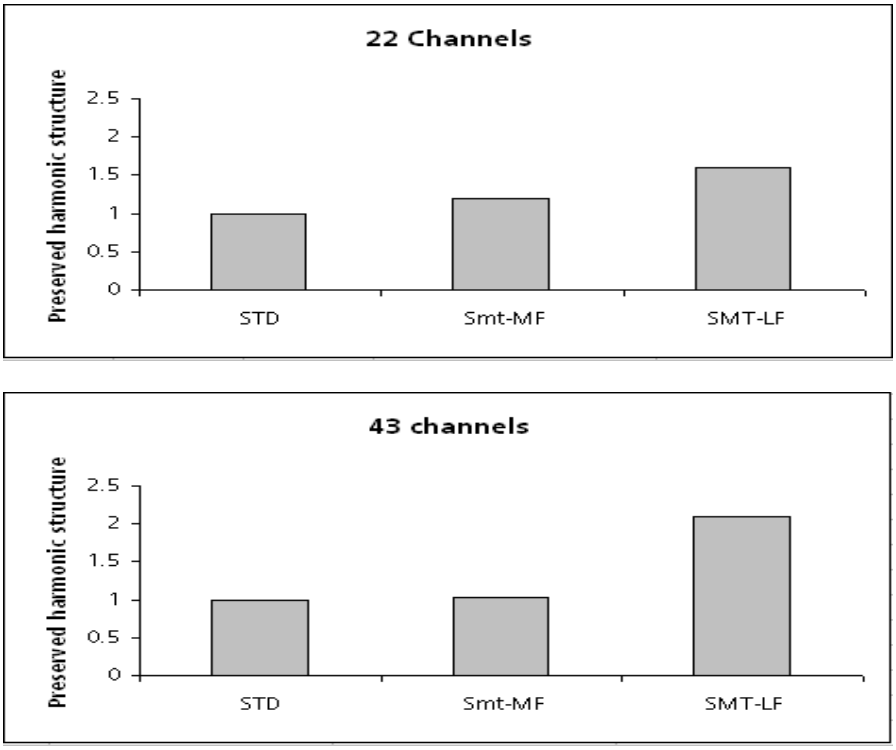

FIGURE 6: Preserved amount of harmonic structure with respect to standard mapping for 22 channels (up) and 43 channels (down).

Figure 6 shows that using 22 and 43 channels the preservation of harmonic structures increase with Smt-MF and increases more with Smt-LF than the Std mapping. In 43 channels the increase between Smt-MF and Std mapping is relatively smaller than of 22 channels, while Smt-LF with 43 channels provides higher preservation of harmonic structure than with 22 channels. Although Smt-LF shows the highest preservation, but it transposes sounds to higher frequencies [1] and patients described it as higher in pitch than similar sounds with Smt-MF [2].

6. DISCUSSION

Music has many descriptions; Heinrich Hueschen (1961) described it among the artistic disciplines and said “it is the one whose material consists of tones. Of the raw materials available in nature, only a small proportion is actually used in music. The finite number of tones selected for musical use from the infinity available in nature is organized into specific tone systems through defined rational processes” [13]. Hans Heinrich Eggebrecht (1967) provided a characterizing definition and said “music is – in the area in which the concept is relevant, western culture – the artistic formation of those sounds that represent the world and the spirit in the form of a voice of nature and emotion in the realm of hearing, concretely conceived, and which achieves significance as an art, become both meaningful and meaning-creating material through reflected and ordered cognition and theory. For the basic element of music, the tone is on one hand the bearer of meaning, while on the other hand it is the vehicle of meaning as the beneficiary of the tonal order. These lend to the unit of music, tone, its specifically cultural forms, meanings and conceptions and at the same time, as a natural phenomenon, it remains accountable to the laws of nature” [14]. Till now there is neither a complete definition of music nor a unit for its underlying

aspects. Rather, various descriptions of the concept that appear in the literature and emphasize a particular aspect of the total phenomenon [9, 13].

Music consists of tones; where a tone is a sound played or sung with a particular pitch and duration. It is one of the important aspects of music. Melody is an agreeable succession of tones that represents a link between the individual musical tone and tonal music as a whole [10]. The sequence of tones in a melody forms its melodic line. Within each melodic line a sequence of oriented intervals defined by neighboring tones can be traced. This sequence demonstrates the movement of the melodic line [15]. Melodies are often described as being made up of phrases. They may also be perceived in short musical ideas (melodic, harmonic, rhythmic or any combination of these three) called motifs [9]. A motif is the smallest meaningful unit, a perceivable or salient recurring fragment or succession of notes that may be used to construct parts of a melody [16]. Long melodies that reappear in a music piece are called themes.

Another two important aspects of music are rhythm and meter. A series of events (whether musical notes or blows of a hammer) is commonly characterized as 'rhythmic' if some or all of those events occur at regular time intervals. Rhythm is a major aspect of music, dance, and most poetry; it involves the pattern of both regular and irregular durations that are present in music. Meter involves the perception and anticipation of rhythm patterns [17]. Meter is a structured attending to time which allows listeners to have precise expectations as to when subsequent musical events are going to occur. It plays a crucial role in the determination of relative durations. Not all durations are perceived the same, as there are a number of psycho-physical limits on the ability to perceive durations and durational succession. Divenyi (1974) demonstrated that two onsets must be separated by at least 2 ms in order to be distinctly perceived, and that at least 15-20 ms are required to determine which onset came first and 100 ms seems to be the threshold for reliable judgments of the length [18]. In rhythm, any periodic transient signal that marks it; is called a beat. Beat may be described as a sudden change in energy with respect to the preceding history. Much music is characterized by the sequence of stressed and unstressed beats [7]. The perception of a beat is not only necessary for a sense of 'connectedness' among successive events; it may also be necessary for a sense of motion [19]. A sense of beat, while necessary, is not sufficient to engender a sense of meter. Timbre is a characteristic feature of musical instruments. Helmholtz was the first person to describe the timbre as a property of the spectral components of the sound [20]. Helmholtz view of timbre was that the perceptual cues came from the Fourier series coefficients. Unlike pitch or rhythm, timbre is developed from many physical features and can not be measured with a scale [7]. Timbre is defined physically by the temporal envelope (particularly the onset) and the spectral shape of the acoustic sound [21]. The characteristics of timbre do not come particularly from the ratio of the strengths of partials, but from the formants.

Harmony is another important aspect of music. The term harmony is derived from the Greek word 'harmonia' and means 'fit or join together'. The term 'harmony' refers to the combination of notes simultaneously to produce chords and successively to produce chord progressions [9]. Chords are groups of notes built on major or minor triads and sounded simultaneously. Sound keeps pleasant to the ear if a musical relationship exists between the overtones of a chord. From the engineering point of view, music can be described as a series of complex acoustic sounds composed of tones. Such tones have a harmonic structure of overtones [4]. Also, harmony can be produced from inharmonic spectrum [7]. An inharmonic spectrum is formed from aperiodic tones; such as frequencies with the "Goldener Schnitt" ratio 1.61803 [22] where the signals in the time domain do not overlap except at t=0.

Acoustic sound in general is described in three domains (loudness, frequency and time). Music has many important aspects and some of them are summarized in Figure 7.

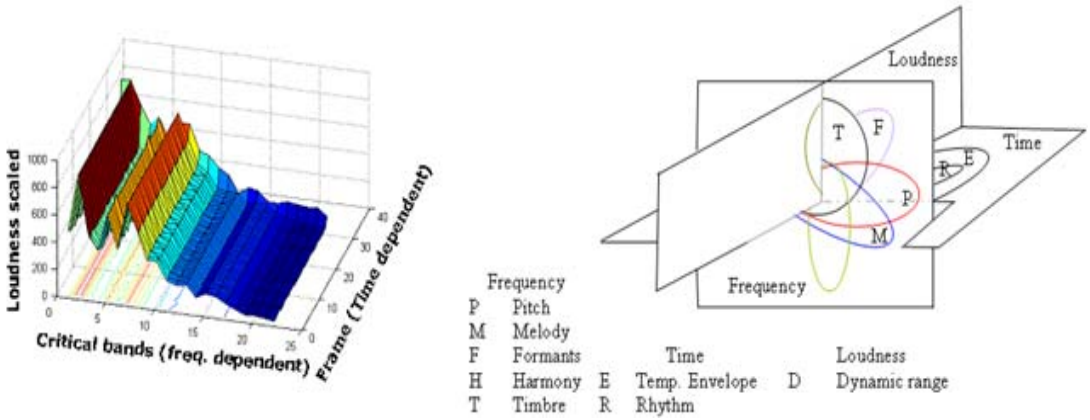

FIGURE 7: Represents a spectro-contrast gram (loudness in Sones scaled along z-axis, critical bands on the x-axis and different frames along y-axis) of a complex clarinet tone in nature. To the right side, different aspects of music are presented categorized according to the three dimensions of sound (frequency, time and loudness).

Up to now, there is no analytical measure of many musical aspects such as the harmony or how appreciated could musical sounds be compared to other processing algorithms. But psychoacoustic tests carried out with either normal hearing subjects through a simulator or CI recipients had proved an enhancement with Smt-MF mapping [2]. However, the proposed method adds a new analytical approach to address this problem. Simulations in Figures (4-5) show clearly that the proposed Semitone mapping which is based on a logarithm semitone scale can enhance representation of musical partials with respect to the current Std mapping algorithm.

On another hand, the proposed method could be used as well in other applications such as robots cameras, mainly in detecting road lines using an index maximization simple matrix rotation and multiplication operations of segregated image parts, which is expected to be effective than currently used methods like Sobel edge detection.

7. CONCLUSION

The O'mat proposed in this paper, proved it can be used to detect diagonal activities in matrices or images, with a detection limitation of the first element (index=1). However, this can be simply compensated with one line of a conditional code. The O'mat algorithm was applied to relatively quantify the amount of harmonic structure preservation with Smt-MF and Smt-LF mappings with respect to the Std mapping for CI devices. Results show that 43 channels provided higher quantity of preservation than 22 channels with Smt-LF mapping. It shows also that the Smt-LF highly ameliorates harmonic structure preservation of overtones in musical notes with respect to Smt-MF mapping which is higher as well than Std mapping.

8. ACKNOWLEDGMENT

This work was partially supported with a scholarship from the University of Zurich. Many thanks to my professors Norbert Dillier and Rodney Douglas.

9. REFERENCES

1. S. Omran, W.K. Lai, N. Dillier. *"Semitone Frequency Maps to Improve Music representation for Nucleus Cochlear Implants"*. Audio speech and music processing journal, submitted, 2011

2. S. Omran, W.K. Lai, N. Dillier. *"Pitch ranking, Melody contour and instrument recognition tests using two semitone frequency maps for Nucleus Cochlear Implants"*. Audio speech and music processing journal, 2010

3. J. Laneau, M. Moonen, J. Wouters. *"Factors affecting the use of noise-band vocoders as acoustic models for pitch perception in cochlear implants"*. J Acoust Soc Am, 119(1):491-506, 2006

4. J. Pierce. *"The science of musical sound"*, Scientific American Books, New York (1983)

5. F. Gantmacher. *"The Theory of Matrices"*, American Mathematical Society, Rhode Island (1990)

6. A. Neubauer. *"Irreguläre Abtastung: Signaltheorie und Signalverarbeitung (Irregular sampling: signal theory and signal processing)"*, Springer Inc, Berlin (2003)

7. M. Neukom. *"Signale, Systeme und Klangsynthesse: Grundlagen der Computermusik (Singals, Systems and Sound synthesis: basics of computer music"*, Peter Lang Inc, Bern (2005)

8. K. Wyatt, C. Schroeder. *"Harmony and Theory: a comprehensive source for all musicians"*, Musicians Institute Press (1998)

9. S. Sadie, G. Grove. *"The New Grove Dictionary of Music and Musicians"*, Grove, London (1995)

10. E. Terhardt. *"Akustische Kommunikation (acoustic communication)"*, Springer-Verlag, Berlin (1998)

11. K. Kasturi, P. Loizou. *"Effect of filter spacing on melody recognition: acoustic and electric hearing"*. J Acoust Soc Am, 122(2):29-34, 2007

12. P.A. Busby, K.L. Plant. *"Dual electrode stimulation using the nucleus CI24RE cochlear implant: electrode impedance and pitch ranking studies"*. Ear Hear, 26(5): 504-515, 2005
13. F. Blume. *"Die Musik in Geschichte und Gegenwart (Music in history and present)"*, Finscher Ludwig (1961)

14. B. Riemann. *"Musik Lexikon (Music lexicon)"*, Direct media Publishing GmbH, Berlin (2000)

15. J. Hofman-Jablan. *"Antisymmetry and colored symmetry of musical work"*. Culture & Science, 6(2): 249-251,1995

16. R. Scruton. *"The Aesthetics of Music"*, Clarendon Press, Oxford (1997)

17. G. Houle. *"Meter in Music, Performance, Perception, and Notation"*, Indiana University Press, pp. 1600-1800 (1987)

18. P.L. Divenyi, I.J. Hirsh. *"Identification of temporal order in three-tone sequences"*. J Acoust Soc Am, 56(1): 144-191, 1974

19. A.S. Bregman. *"Auditory Scene Analysis: The Perceptual Organization of sound"*, The MIT Press, Cambridge, Massachusetts (1990)

20. H.L.F. Helmholtz. *"On the Sensations of Tone as a Physiological Basis for the Theory of Music"*, New York Dover (1954)

21. S. Handel. *"Timbre perception and auditory object formation"*, Academic Press, San Diego (CA). pp. 425-461 (1995)

22. H. Walser. *“Der Goldene Schnitt (The Golden Schnitt)”*. Teubner, Stuttgart (1993)

CALL FOR PAPERS

Journal: International Journal of Robotics and Automation (IJRA)
Volume: 2 **Issue:** 1
ISSN:2180-1312
URL: http://www.cscjournals.org/csc/description.php?JCode=IJRA

About IJRA

Robots are becoming part of people's everyday social lives - and will increasingly become so. In future years, robots may become caretaking assistants for the elderly, or academic tutors for our children, or medical assistants, day care assistants, or psychological counselors. Robots may become our co-workers in factories and offices, or maids in our homes.

The International Journal of Robotics and Automation (IJRA), a refereed journal aims in providing a platform to researchers, scientists, engineers and practitioners throughout the world to publish the latest achievement, future challenges and exciting applications of intelligent and autonomous robots. IJRA is aiming to push the frontier of robotics into a new dimension, in which motion and intelligence play equally important roles. IJRA scope includes systems, dynamics, control, simulation, automation engineering, robotics programming, software and hardware designing for robots, artificial intelligence in robotics and automation, industrial robots, automation, manufacturing, and social implications.

To build its International reputation, we are disseminating the publication information through Google Books, Google Scholar, Directory of Open Access Journals (DOAJ), Open J Gate, ScientificCommons, Docstoc and many more. Our International Editors are working on establishing ISI listing and a good impact factor for IJRA.

IJRA List of Topics

The realm of International Journal of Robotics and Automation (IJRA) extends, but not limited, to the following:

- Automation Control
- Autonomous Robots
- Emergence of The Thinking Machine
- Household Robots and Automation
- Jacobian and Singularities
- Nanotechnology & Robotics (Nanobots)
- Robot Controller
- Automation Engineering
- Biotechnology & Robotics
- Forward Kinematics
- Inverse Kinematics
- Methods for Teaching Robots
- Orientation Matrices
- Robot Structure and Workspace

- Robotic & Automation Software Development
- Robotic Exploration
- Robotic Surgery
- Robotic Surgical Procedures
- Robotic Welding
- Robotics Applications
- Robotics Programming
- Robotics Technologies
- Robots Society and Ethics
- Software and Hardware Designing for Robots
- Spatial Transformations
- Trajectory Generation
- Unmanned (Robotic) Vehicles

IMPORTANT DATES

Volume: 2
Issue: 1
Paper Submission: January 31, 2011
Author Notification: March 01, 2011
Issue Publication: March / April 201

CALL FOR EDITORS/REVIEWERS

CSC Journals is in process of appointing Editorial Board Members for ***International Journal of Robotic and Automation (IJRA)***. CSC Journals would like to invite interested candidates to join ***IJRA*** network of professionals/researchers for the positions of Editor-in-Chief, Associate Editor-in-Chief, Editorial Board Members and Reviewers.

The invitation encourages interested professionals to contribute into CSC research network by joining as a part of editorial board members and reviewers for scientific peer-reviewed journals. All journals use an online, electronic submission process. The Editor is responsible for the timely and substantive output of the journal, including the solicitation of manuscripts, supervision of the peer review process and the final selection of articles for publication. Responsibilities also include implementing the journal's editorial policies, maintaining high professional standards for published content, ensuring the integrity of the journal, guiding manuscripts through the review process, overseeing revisions, and planning special issues along with the editorial team.

A complete list of journals can be found at http://www.cscjournals.org/csc/byjournal.php. Interested candidates may apply for the following positions through http://www.cscjournals.org/csc/login.php.

Please remember that it is through the effort of volunteers such as yourself that CSC Journals continues to grow and flourish. Your help with reviewing the issues written by prospective authors would be very much appreciated.

Feel free to contact us at coordinator@cscjournals.org if you have any queries.

Contact Information

Computer Science Journals Sdn BhD
M-3-19, Plaza Damas Sri Hartamas
50480, Kuala Lumpur MALAYSIA

Phone: +603 6207 1607
+603 2782 6991
Fax: +603 6207 1697

BRANCH OFFICE 1
Suite 5.04 Level 5, 365 Little Collins Street,
MELBOURNE 3000, Victoria, AUSTRALIA

Fax: +613 8677 1132

BRANCH OFFICE 2
Office no. 8, Saad Arcad, DHA Main Bulevard
Lahore, PAKISTAN

EMAIL SUPPORT
Head CSC Press: coordinator@cscjournals.org
CSC Press: cscpress@cscjournals.org
Info: info@cscjournals.org

COMPUTER SCIENCE JOURNALS SDN BHD
M-3-19, PLAZA DAMAS
SRI HARTAMAS
50480, KUALA LUMPUR
MALAYSIA